nature neuroscience

TECHNICAL REPORT

https://doi.org/10.1038/s41593-021-00823-7

Check for updates

A genetically encoded sensor for measuring serotonin dynamics

Jinxia Wan[1,2], Wanling Peng[3], Xuelin Li[1,2], Tongrui Qian[1,2], Kun Song[3], Jianzhi Zeng[1,2,4], Fei Deng[1,2], Suyu Hao[1,2], Jiesi Feng[1,2,4], Peng Zhang[5], Yajun Zhang[5], Jing Zou[1,2,6], Sunlei Pan[1,2,4], Mimi Shin[7], B. Jill Venton[7], J. Julius Zhu[5], Miao Jing[8], Min Xu[3] and Yulong Li[1,2,4] ✉

Serotonin (5-HT) is a phylogenetically conserved monoamine neurotransmitter modulating important processes in the brain. To directly visualize the release of 5-HT, we developed a genetically encoded G-protein-coupled receptor (GPCR)-activation-based 5-HT ($GRAB_{5\text{-}HT}$) sensor with high sensitivity, high selectivity, subsecond kinetics and subcellular resolution. $GRAB_{5\text{-}HT}$ detects 5-HT release in multiple physiological and pathological conditions in both flies and mice and provides new insights into the dynamics and mechanisms of 5-HT signaling.

Serotonergic signaling in the brain plays a critical role in a wide range of physiological processes, including mood control, reward processing and sleep–wake homeostatic regulation[1–3]. Indeed, drugs targeting central serotonergic activity have been used to treat virtually every psychiatric disorder, with the best example being the use of selective 5-HT reuptake inhibitors for depression[4]. Yet, despite the importance of 5-HT, our understanding of cell-specific 5-HT signaling during behaviors is very much lacking, in part due to our inability to measure 5-HT in vivo with high sensitivity and spatiotemporal resolution[5–7]. Here, using molecular engineering, we developed a genetically encoded fluorescent sensor for directly measuring extracellular 5-HT.

Results

Development and characterization of the $GRAB_{5\text{-}HT1.0}$ sensor in cultured cells. Previously, we and others independently developed GPCR-activation-based (GRAB) sensors for detecting different neurotransmitters by converting the conformational change in the respective GPCR to a sensitive fluorescence change in the circular permutated GFP (cpGFP)[8–11]. Using a similar strategy, we initiated the engineering of 5-HT-specific sensors by inserting a cpGFP into the third intracellular loop of various 5-HT receptors. Based on the performance of membrane trafficking and the affinity of receptor–cpGFP chimeras, we selected the 5-HT2C receptor-based chimera for further optimization (Extended Data Fig. 1a,b). Our previous experience in optimizing GRAB sensors[8,10,11] shows that the N- and C-terminal linkers between GPCR and cpGFP are critical for the sensor's performance. Therefore, we randomly mutated five sites in both the N-terminal and C-terminal linkers between the 5-HT2C receptor and cpGFP to improve the response of the 5-HT sensor. Moreover, we introduced mutations into the cpGFP, focusing on sites that are potentially critical for fast GFP folding and high levels of brightness[12,13] (Extended Data Fig. 2). Mutagenesis and screening in the linker regions and the cpGFP moiety resulted in a sensor with a 250% change in fluorescence ($\Delta F/F_0$) in response to 5-HT in cultured HEK293T cells, which we named $GRAB_{5\text{-}HT1.0}$ (referred to hereafter as simply 5-HT1.0; Fig. 1a and Extended Data Fig. 3). In addition, we generated a 5-HT-insensitive version of this sensor by introducing the $D134^{3.32}Q$ substitution into the receptor[14,15] ($GRAB_{5\text{-}HTmut}$, referred to hereafter as 5-HTmut; Fig. 1 and Extended Data Fig. 4). This mutant sensor showed similar membrane trafficking as that of 5-HT1.0 (Extended Data Fig. 4a) but had <2% $\Delta F/F_0$ even in the presence of 100 μM 5-HT (Fig. 1a and Extended Data Fig. 4a–d). In cultured rat cortical neurons, the 5-HT1.0 sensor produced a robust increase in fluorescence (280% $\Delta F/F_0$) in both the soma and neurites in response to bath application of 5-HT, whereas the 5-HTmut sensor had no measurable change in fluorescence (Fig. 1b and Extended Data Fig. 4n).

Next, we characterized the properties of the 5-HT1.0 sensor in detail. Specifically, we measured the brightness, photostability, the dose–response curve, response kinetics, signal specificity and downstream coupling of this sensor. We found that the 5-HT1.0 sensor had brightness similar to and better photostability than enhanced (E)GFP in the presence of 5-HT (Extended Data Fig. 4e–g). Regarding the sensor's kinetics, the τ_{on} and τ_{off} values were around 0.2 s and 3.1 s, respectively, as measured by applying 5-HT (to measure the on rate τ_{on}), followed by the 5-HT receptor antagonist metergoline (Met, to measure the off rate τ_{off}) in cultured HEK293T cells (Fig. 1c). In addition, the 5-HT1.0 sensor was highly sensitive to 5-HT, with a half-maximal effective concentration (EC_{50}) of 22 nM (Fig. 1e). None of the other tested neurotransmitters or neuromodulators elicited a detectable fluorescence change. Importantly, the 5-HT-induced signal was eliminated by the specific 5-HT2C receptor antagonist SB-242084 (SB) (Fig. 1d and Extended Data Fig. 4o,p), indicating a high specificity for 5-HT. Moreover, unlike the native 5-HT2C receptor, which couples to intracellular G protein and β-arrestin signaling pathways, the 5-HT1.0 sensor showed no detectable coupling to either of these two pathways, as measured by calcium imaging, cAMP imaging[16], the G protein-dependent luciferase

[1]State Key Laboratory of Membrane Biology, Peking University School of Life Sciences, Beijing, China. [2]PKU-IDG/McGovern Institute for Brain Research, Beijing, China. [3]Institute of Neuroscience, State Key Laboratory of Neuroscience, CAS Center for Excellence in Brain Science and Intelligence Technology, Chinese Academy of Sciences, Shanghai, China. [4]Peking-Tsinghua Center for Life Sciences, Academy for Advanced Interdisciplinary Studies, Peking University, Beijing, China. [5]Department of Pharmacology, University of Virginia School of Medicine, Charlottesville, VA, USA. [6]Department of Biological Sciences, Neurobiology Section, University of Southern California, Los Angeles, CA, USA. [7]Department of Chemistry, University of Virginia, Charlottesville, VA, USA. [8]Chinese Institute for Brain Research, Beijing, China. ✉e-mail: yulongli@pku.edu.cn

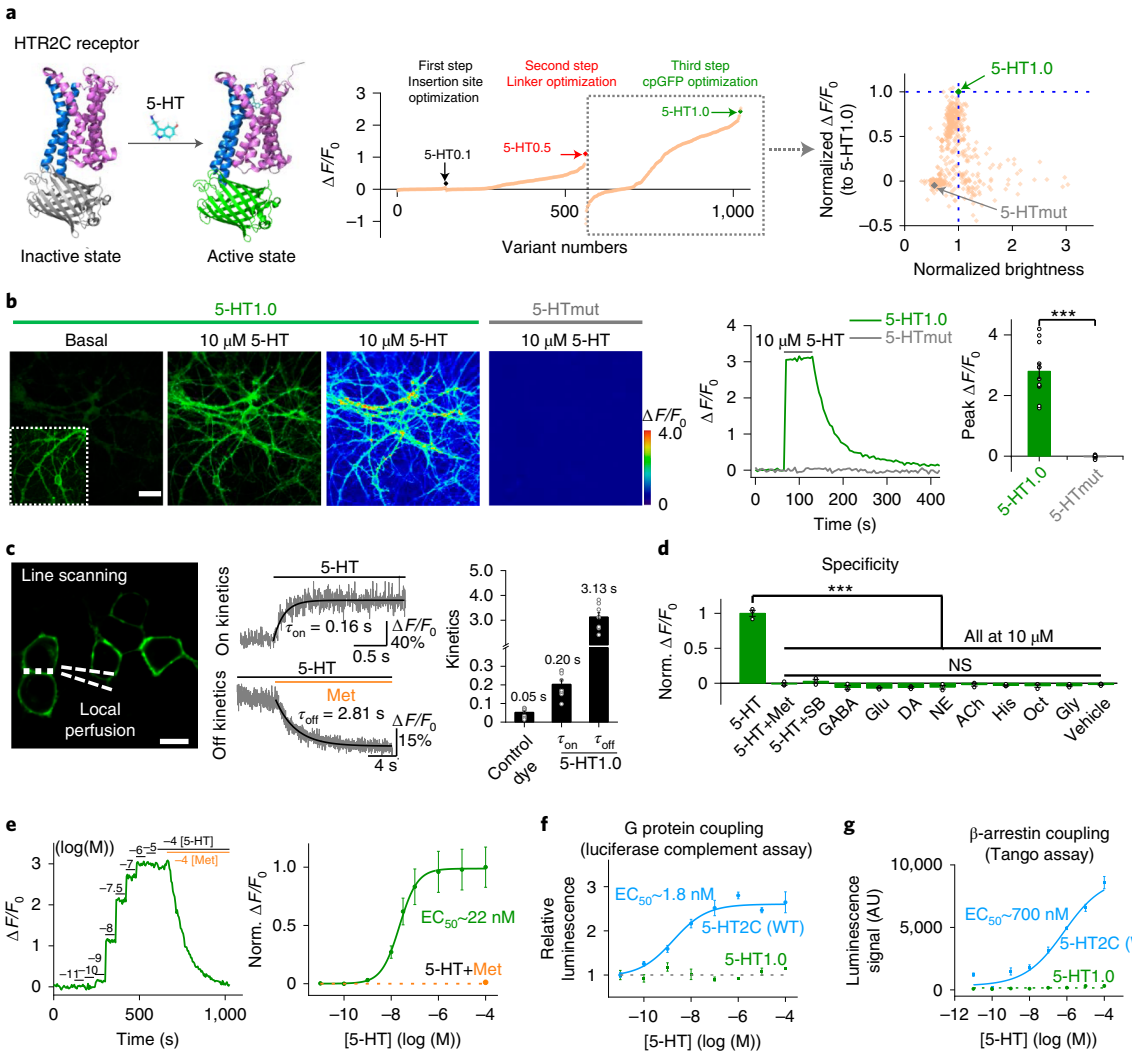

Fig. 1 | Design, optimization and characterization of a new genetically encoded 5-HT sensor. a, Left: schematic representation illustrating the principle behind the $GRAB_{5\text{-}HT}$ sensor. Crystal structures are from the Protein Data Bank (PDB) archive (PDB IDs 6BQH and 6BQG for the inactive and active states of the 5-HT2C receptor, respectively[14] and PDB ID 3EVP for cpGFP[32]). Middle: the 5-HT sensor was optimized over three main steps, including those targeting the cpGFP insertion site, the linker between cpGFP and the 5-HT2C receptor and critical amino acids in cpGFP. Right: optimization of cpGFP and engineering of 5-HTmut. The fluorescence change in each candidate sensor is plotted against the brightness, with both axes normalized to 5-HT1.0. **b**, Representative images (left), fluorescence response traces (middle) and group data (right) of the fluorescence response in cultured rat cortical neurons expressing 5-HT1.0 (green) or 5-HTmut (gray); when indicated, 10 μM 5-HT was applied. The inset in the left fluorescence image shows the region with increased contrast; $n = 12$ cells from three cultures (hereafter denoted as 12/3) for each group. A two-tailed Student's *t*-test was performed. $P = 1.65 \times 10^{-7}$ for 5-HT1.0 versus 5-HTmut. Scale bar, 20 μm. **c**, Kinetic analysis of the 5-HT1.0 sensor in cultured HEK293T cells. Left: a representative image showing the experimental protocol, in which the line-scanning mode was used to record the fluorescence change in HEK293T cells expressing 5-HT1.0 in response to local application of 5-HT, followed by application of Met in the continued presence of 5-HT. Middle: representative traces showing the increase and decrease in 5-HT1.0 fluorescence in response to 5-HT (top) followed by Met (bottom). Right: a summary of on and off kinetics of 5-HT1.0; $n = 10/3$, 8/3 and 8/3 for control dye, τ_{on} and τ_{off} groups. Scale bar, 10 μm. **d**, Summary of the change in fluorescence of 5-HT1.0 in response to 5-HT alone, 5-HT together with Met or SB and eight additional neurotransmitters and neuromodulators. Glu, glutamate; DA, dopamine; NE, norepinephrine; ACh, acetylcholine; His, histamine; oct, octopamine; and Gly, glycine; $n = 3$ wells per group with 300–500 cells per well. Two-tailed Student's *t*-tests were performed. $P = 2.67 \times 10^{-5}$, 4.44×10^{-5}, 3.01×10^{-5}, 1.73×10^{-5}, 1.89×10^{-5}, 2.97×10^{-5}, 2.74×10^{-5}, 2.00×10^{-5}, 2.91×10^{-5}, 2.16×10^{-5} and 2.09×10^{-5} for 5-HT versus 5-HT and Met, 5-HT and SB, GABA, Glu, dopamine, norepinephrine, acetylcholine, His, octopamine, Gly and vehicle, respectively. $F_{10,22} = 2.25$, $P = 0.0546$ for 5-HT and Met, 5-HT and SB, GABA, Glu, dopamine, norepinephrine, acetylcholine, His, octopamine, Gly and vehicle by one-way ANOVA. Norm., normalized. **e**, The dose–response curve was measured in neurons expressing 5-HT1.0 in response to increasing concentrations (indicated with square brackets) of 5-HT, followed by the addition of Met; $n = 18/4$ for each group. G protein coupling (**f**) and β-arrestin coupling (**g**) were measured for the 5-HT1.0 sensor and the 5-HT2C receptor using a luciferase complementation assay and a Tango assay, respectively; $n = 3$ wells per group with 100–300 cells per well. AU, arbitrary units; WT, wild type. Data are shown as mean ± s.e.m. in **b**–**g**, with the error bars or shaded regions indicating the s.e.m., $^{***}P < 0.001$ and NS, not significant.

complementation assay[17], the Tango assay[18] and long-term measurements of membrane fluorescence in the presence of 5-HT (Fig. 1f,g and Extended Data Fig. 4h–l). Additionally, the expression of 5-HT1.0 did not alter 5-HT2C receptor coupling with the G protein (Extended Data Fig. 4m), indicating that the 5-HT1.0 sensor has little effect on the activation of the wild-type 5-HT2C receptor.

Detecting 5-HT release in mouse brain slices and *Drosophila* with the GRAB$_{5\text{-HT1.0}}$ sensor. Having validated the sensor in cultured cells, to determine whether 5-HT1.0 could function well in mouse brain slices, we expressed 5-HT1.0 using adeno-associated virus (AAV) in the mouse hippocampus, which receives innervation from serotonergic neurons. The 5-HT1.0 sensor showed an increase in fluorescence of more than 100% in individual somata and neurites when 5-HT was exogenously applied (Extended Data Fig. 5a–d). In addition, we also expressed either 5-HT1.0 or 5-HTmut in the mouse dorsal raphe nucleus (DRN) by using AAVs (Fig. 2a). The DRN is the largest serotonergic nucleus in the brain and provides extensive projections to various brain regions[19]. In DRN slices expressing 5-HT1.0, a single electrical pulse evoked detectable increases in fluorescence, and the response was progressively enhanced with increases in pulse number or frequency (Fig. 2b,c and Extended Data Fig. 5e). The stimulation-evoked response was repeatable for up to 25 min (Extended Data Fig. 5f) and blocked by the 5-HT receptor antagonist Met but not by the dopamine receptor antagonist haloperidol (Halo; Fig. 2d and Extended Data Fig. 5g,h). By contrast, the same electrical stimuli did not affect fluorescence in DRN expressing the 5-HTmut sensor (Fig. 2b,d). We also measured the kinetics of the fluorescence change in response to 100-ms electrical stimulation and found τ_{on} and τ_{off} values of approximately 0.15 s and 7.22 s (Fig. 2e). We further compared the 5-HT1.0 sensor with existing fast-scan cyclic voltammetry (FSCV) in recording 5-HT by simultaneously conducting fluorescence imaging and electrochemical recording in DRN slices (Fig. 2f). Both methods could sensitively detect the single pulse-evoked 5-HT signal and the increase in response following incremental frequencies (Fig. 2g and Extended Data Fig. 5i,j). The 5-HT1.0 sensor showed a better signal-to-noise ratio (SNR) than did FSCV (Fig. 2g). In sum, these results show that the 5-HT1.0 sensor has the ability to measure electrically induced endogenous 5-HT release ex vivo.

We next tested whether the 5-HT1.0 sensor could be used to measure sensory-relevant changes in 5-HT signaling in vivo. To this end, we first used the *Drosophila* model, as 5-HT is released from single serotoninergic dorsal paired medial (DPM) neurons that innervate Kenyon cells (KCs) in the mushroom body (MB) of each hemisphere[20,21] and serotonergic signaling in the MB was implicated in odor-related memory consolidation[22]. We expressed the 5-HT1.0 sensor in KCs and found that the sensor reliably reported 5-HT release evoked by electrical stimulation of the horizontal lobe of the MB with rapid on and off kinetics of ~0.07 s and ~4.08 s, respectively. Moreover, the signal was blocked by applying Met (Fig. 2h–j and Extended Data Fig. 6a–c). To determine whether the sensor could report physiologically relevant 5-HT release from a single cell, we directly expressed the 5-HT1.0 sensor either in a single presynaptic serotonergic DPM neuron or in postsynaptic KCs. Consistent with a previous calcium imaging study in the DPM[23], the 5-HT1.0 sensor in either DPM neurons or KCs could report 5-HT release in the MB β′ lobe in response to odor application or body shock (Fig. 2k–q, Extended Data Fig. 6d–i and Supplementary Video 1). By contrast, no fluorescence change was detected in flies expressing the 5-HTmut sensor (Extended Data Fig. 6d–i and Supplementary Video 1). Neither odor application nor body shock produced a saturated response of the 5-HT1.0 sensor, as application of exogenous 5-HT at 100 μM in the same flies elicited much larger responses (Extended Data Fig. 6d–i). When we coexpressed the 5-HT1.0 sensor together with a red fluorescent calcium sensor, jRCaMP1a, in KCs, two-color imaging showed that odorant application

Fig. 2 | GRAB$_{5\text{-HT}}$ can report the release of endogenous 5-HT in acute mouse brain slices and *Drosophila*. **a**, Schematic illustration depicting mouse brain slice experiments. Top: the AAV vector was used to express the 5-HT1.0 sensor. Bottom: AAV expressing either 5-HT1.0 or 5-HTmut was injected in the mouse DRN, after which acute brain slices were prepared and recorded. ITR, inverted terminal repeat; WPRE, woodchuck hepatitis post-transcriptional regulatory element. **b**, Representative fluorescence images of 5-HT1.0, pseudocolor images of the fluorescence change in 5-HT1.0 and 5-HTmut in response to the indicated electrical stimuli delivered at 20 Hz. The duration of one pulse was 1 ms. The white dashed circle (50 μm in diameter) indicates the region of interest used for further analysis. Similar results were observed for 2–5 mice. Scale bar, 50 μm. Stim, stimulation. **c**, Individual traces (left) and quantification (right) of the change in 5-HT1.0 fluorescence in response to the indicated electrical stimuli delivered at 20 Hz; $n = 8$ slices from five mice. **d**, Representative traces (left) and group data (right) of the changes in 5-HT1.0 and 5-HTmut fluorescence in response to electrical stimulation of slices treated with the dopamine receptor antagonist Halo or the 5-HT receptor antagonist Met; $n = 5$ slices from four mice for the 5-HT1.0 group, $n = 3$ slices from one mouse for the 5-HTmut group. Two-tailed Student's *t*-tests were performed. $P = 0.340$ for 5-HT1.0 in artificial cerebrospinal fluid (ACSF) versus Halo; $P = 1.47 \times 10^{-5}$ for 5-HT1.0 in ACSF versus Met; $P = 2.18 \times 10^{-5}$ for 5-HT1.0 in ACSF versus 5-HTmut in ACSF. **e**, Left: changes in normalized (norm.) fluorescence of 5-HT1.0 in response to ten electrical stimuli delivered at 100 Hz. The rise and decay phases are fitted with single-exponential functions (black traces). A magnified view of the on kinetics is shown in the inset. Right, summary of τ_{on} and τ_{off} values; $n = 5$ slices from four mice. **f**, Schematic drawing outlining the design of simultaneous imaging and FSCV experiments in mouse DRN slice preparations. The red arrow indicates that the carbon-fiber microelectrode (CFME) was placed near the neuron expressing 5-HT1.0. Scale bar, 20 μm. **g**, Left: representative fluorescence traces of a DRN neuron expressing 5-HT1.0 after electrical stimulation consisting of a train of 20 pulses at varied frequencies. Middle: current versus time traces of evoked 5-HT release at varied stimulating frequencies. Right: group summary of the SNR of 5-HT1.0 and FSCV; $n = 11$ neurons from nine mice. Two-tailed Student's *t*-tests were performed. $P = 0.0784$, 0.0507, 0.112, 0.0936, 0.0252, 0.00647 and 0.00272 for 1 Hz, 2 Hz, 4 Hz, 8 Hz, 16 Hz, 32 Hz and 64 Hz, respectively. **h**, Left: a schematic drawing showing in vivo two-photon imaging of a *Drosophila* specimen, with the stimulating electrode positioned near the MB. Middle and right: representative images of a fly expressing 5-HT1.0 in KCs of the MB; the image on the right is a magnified view of the dashed rectangle. The duration of one pulse was 1 ms. Similar results were observed for eight flies. Scale bar, 10 μm. 2PM, two-photon microscope. **i**, Representative traces (left) and group analysis (right) of 5-HT1.0 fluorescence in response to the indicated electrical stimuli with either saline (control) or 10 μM Met; $n = 8$ flies for each group. Two-tailed Student's *t*-tests were performed. $P = 2.36 \times 10^{-5}$ for saline versus Met. **j**, Summary of 5-HT1.0 τ_{on} and τ_{off} values in response to a single electrical stimulation; $n = 8$ flies for each group. **k**,**l**, Cartoon and immunostaining images of DPM neurons. Cartoon of the DPM neurons in the MB (**k**) and immunostaining images of the soma of DPM neurons (**l**, left) and neuropil (**l**, right) in the MB region. Similar results were observed for five flies. Scale bar, 50 μm. **m**, Representative image of a fly expressing 5-HT1.0 in the single serotonergic DPM neuron in the fly MB region of one hemisphere. Similar results were observed for more than ten flies. Scale bar, 10 μm. **n**–**p**, Representative pseudocolor images (left) and traces (right) of 5-HT1.0 in the MB β′ lobe in response to odor application for 1 s (**n**), a 0.5-s body shock (**o**) and perfusion with 100 μM 5-HT (**p**). **q**, Group analysis of 5-HT1.0 in response to different stimuli. $n = 13$ flies for odor and body-shock groups, $n = 11$ flies for the perfusion group. **r**–**t**, Representative fluorescence images (top), fluorescence response traces (bottom) (**r**,**s**) and group summary (**t**) of jRCaMP1a in fly MB with coexpression of 5-HT1.0 (**r**) or expression of jRCaMP1a alone (**s**) in KCs in response to odorant stimulation for 1 s. Scale bar, 10 μm. $n = 11$ and $n = 10$ flies for the jRCaMP1a response in 5-HT1.0$^+$ and 5-HT1.0$^-$ groups; $n = 11$ and $n = 9$ flies for the 5-HT1.0 response in 5-HT1.0$^+$ and 5-HT1.0$^-$ groups. Two-tailed Student's *t*-tests were performed. $P = 0.179$ and $P = 2.15 \times 10^{-9}$ for jRCaMP1a and 5-HT1.0 peak responses. Data are shown as mean ± s.e.m. in **c**–**e**,**g**,**i**,**j**,**q**–**t**, with the error bars or shaded regions indicating the s.e.m., $^*P < 0.05$, $^{**}P < 0.01$ and $^{***}P < 0.001$.

increased both the 5-HT1.0-mediated green 5-HT fluorescence and the jRCaMP1a-mediated red calcium fluorescence responses (Fig. 2r–t). Moreover, jRCaMP1a-expressing flies with or without coexpression of 5-HT1.0 had similar odorant-evoked calcium signals, suggesting little effect of 5-HT1.0 sensor expression on neuronal calcium activities (Fig. 2r–t and Extended Data Fig. 6j,k).

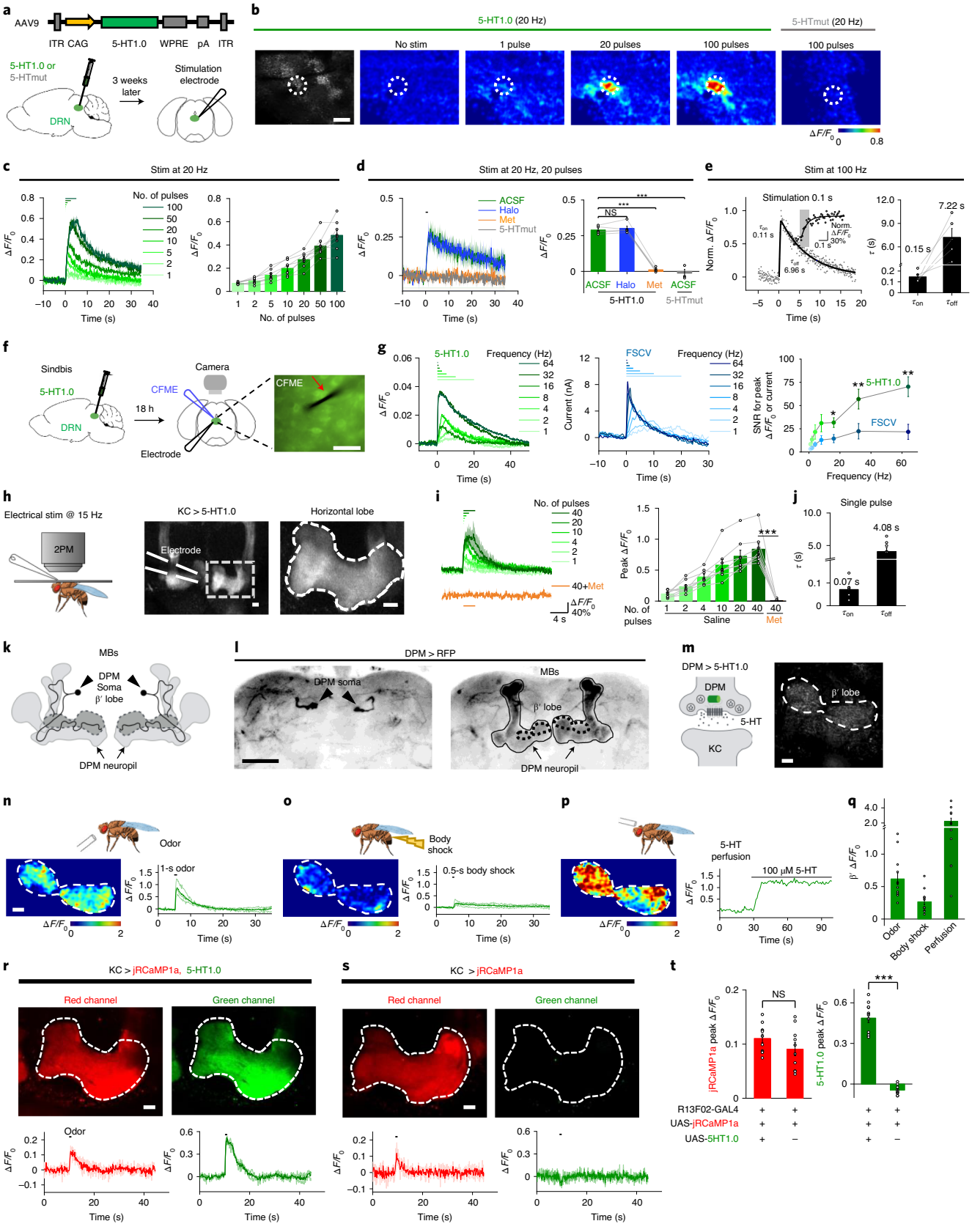

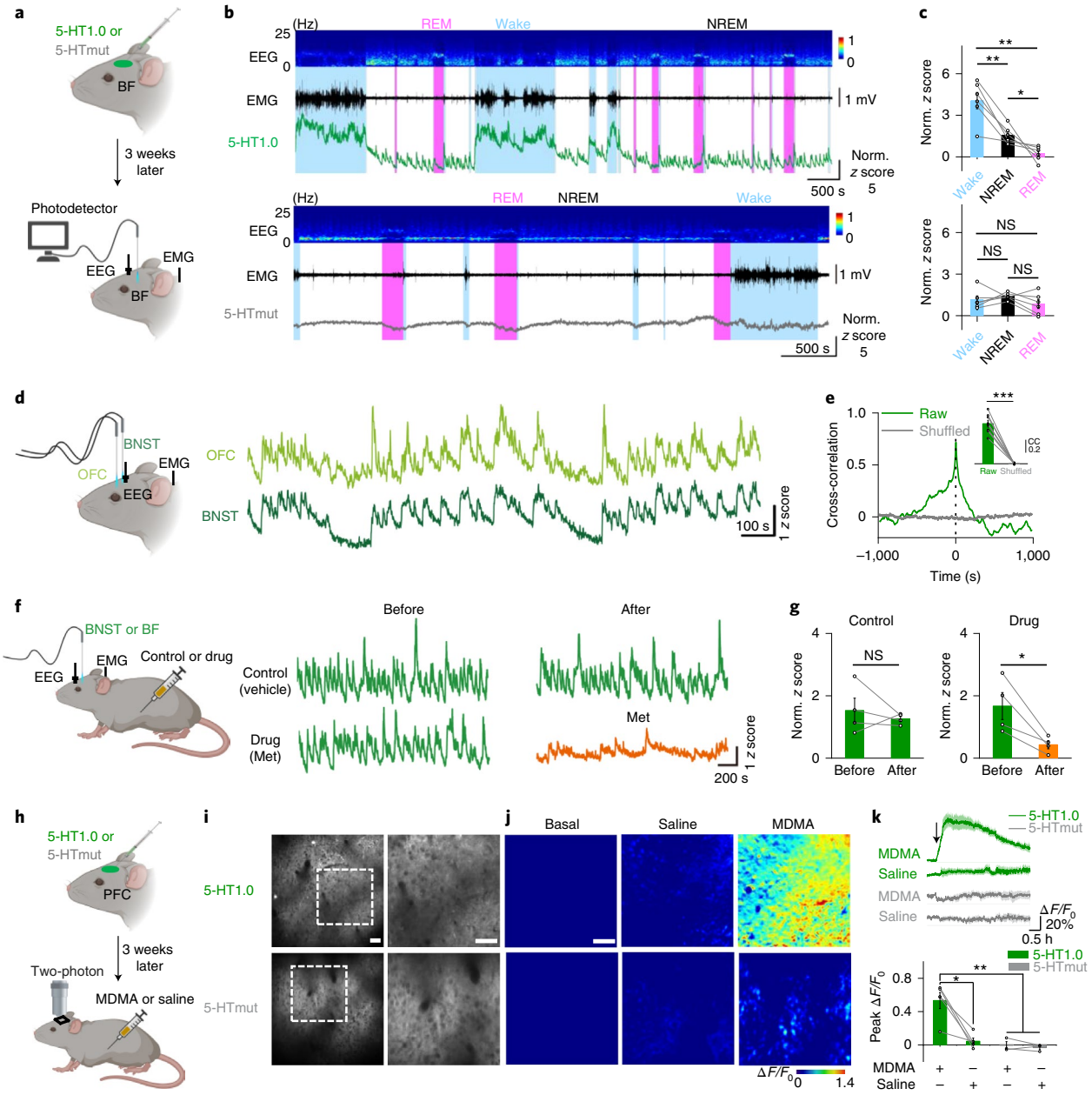

Fig. 3 | GRAB$_{5\text{-HT}}$ can report endogenous serotonergic activity in freely behaving mice. a, Schematic diagram illustrating the use of fiber photometry for measuring 5-HT1.0 and 5-HTmut fluorescence in the BF of freely behaving mice during the sleep–wake cycle. EEG and EMG were also performed. **b**, Representative EEG, EMG and 5-HT1.0 (top) and 5-HTmut (bottom) fluorescence measured during the sleep–wake cycle. The REM sleep state is shaded pink, and the waking state is shaded light blue. Similar results were observed for three mice. **c**, Summary of 5-HT1.0 (top) and 5-HTmut (bottom) fluorescence measured in awake mice and during NREM and REM sleep; $n = 3$ mice in two sessions for each group. Two-tailed Student's t-tests were performed. For 5-HT1.0, $P = 0.00382$ for awake versus NREM, $P = 0.00374$ for awake versus REM and $P = 0.0334$ for NREM versus REM. For 5-HTmut, $P = 0.474$ for awake versus NREM, $P = 0.255$ for awake versus REM and $P = 0.107$ for NREM versus REM. **d**,**e**, Same as in **a**, except that the 5-HT1.0 sensor was expressed in both the OFC (light green) and the BNST (dark green), and the fluorescence response in each nucleus was recorded and analyzed. Similar results were observed for four mice. The cross-correlation (CC) between the signals in the OFC and the BNST is shown in **e**; $n = 4$ mice in two sessions for each group. A two-tailed Student's t-test was performed. $P = 8.72 \times 10^{-6}$ for raw versus shuffled groups. **f**,**g**, 5-HT1.0 fluorescence was measured in the BNST and the BF as shown in **f**; when indicated, mice received an injection of saline (control) or Met. Normalized responses in the BNST ($n = 3$ mice) and the BF ($n = 1$ mouse) were combined for the group summary. Two-tailed Student's t-tests were performed. $P = 0.533$ and $P = 0.0361$ for control and drug groups. **h**, Schematic diagram illustrating the use of two-photon imaging to measure 5-HT1.0 and 5-HTmut fluorescence in the PFC of head-fixed mice; MDMA or saline was i.p. injected. **i**, Representative fluorescence images of 5-HT1.0 (top, left) and 5-HTmut (bottom, left) measured in the mouse PFC. The images on the right are the corresponding magnified views of the dashed boxes on the left. Similar results were observed for more than three mice. Scale bar, 50 µm. **j**,**k**, Representative pseudocolor images (**j**), averaged fluorescence traces (**k**, top) and a group summary (**k**, bottom) showing changes in 5-HT1.0 (top, green) and 5-HTmut (bottom, gray) fluorescence after an i.p. injection of saline (middle) or MDMA at 10 mg per kg (right); $n = 5$ mice for the 5-HT1.0 group, $n = 3$ mice for the 5-HTmut group. Two-tailed Student's t-tests were performed. $P = 0.0106$ for 5-HT1.0 with MDMA versus 5-HT1.0 with saline; $P = 0.00669$ for 5-HT1.0 with MDMA versus 5-HTmut with MDMA; $P = 0.00477$ for 5-HT1.0 with MDMA versus 5-HTmut with saline. Scale bar, 50 µm. Data are shown as mean ± s.e.m. in **c**,**e**,**g**,**k**, with the error bars or shaded regions indicating the s.e.m., $^{*}P < 0.05$, $^{**}P < 0.01$ and $^{***}P < 0.001$.

Monitoring endogenous 5-HT dynamics in mice in vivo. Following this, we examined whether the 5-HT1.0 sensor could measure the dynamics of serotonergic activity under physiological conditions in mice, such as during the sleep–wake cycle. The basal forebrain (BF), the orbital frontal cortex (OFC) and the bed nucleus of the stria terminalis (BNST) not only participate in the regulation of sleep and wake cycles but also receive extensive DRN serotonergic projections[24,25]. Hence, we expressed the 5-HT1.0 sensor in these brain regions and then performed simultaneous fiber photometry and electroencephalography (EEG) and electromyography (EMG) recordings in freely behaving mice. The BF 5-HT1.0 sensor signal was generally higher during waking than that during sleep. Comparing rapid-eye-movement (REM) sleep and non-REM (NREM) sleep, the signal was lower during REM sleep, consistent with previous findings[26] (Fig. 3a–c). As expected, we found no substantial change in fluorescence in mice expressing the 5-HTmut sensor during the sleep–wake cycle (Fig. 3a–c). Interestingly, simultaneous recordings of 5-HT1.0 in the OFC and the BNST revealed a tight correlation in fluorescence during NREM sleep (Fig. 3d,e), suggesting global synchrony of 5-HT signaling despite region-specific innervation by different subpopulations of serotonergic neurons in the DRN[25,27]. Lastly, consistent with our previous findings, we found that treating mice with the 5-HT receptor antagonist Met largely blocked fluorescence changes of the 5-HT1.0 sensor (Fig. 3f,g), validating the specificity of measured signals in vivo.

Finally, to determine whether the sensor could reveal the action of psychostimulant drugs, we used methylenedioxymethamphetamine (MDMA), which is a synthetically addictive compound that can alter mood and perception; its effects are partially attributed to an increase in extracellular 5-HT concentrations in the brain[28]. We examined the effect of MDMA in vivo by two-photon imaging of mice expressing the sensor in the prefrontal cortex (PFC), a higher cognitive region that receives abundant serotonergic innervation[29]. Intraperitoneal (i.p.) injection of MDMA caused a gradual increase in 5-HT1.0 fluorescence, which peaked after 1 h and then gradually decayed over the following 3 h (Fig. 3h–k). This time course is comparable with that of the psychostimulation effect of MDMA in both humans[30] and mice[31]. Meanwhile, MDMA had no effect on the fluorescence of the 5-HTmut sensor (Fig. 3h–k). These results together suggest that the 5-HT1.0 sensor is suitable for stable and long-term imaging in vivo.

Discussion

In summary, we report the development and application of a new genetically encoded fluorescent GRAB sensor for measuring extracellular 5-HT dynamics. The newly developed $GRAB_{5\text{-}HT1.0}$ sensor shows a high affinity for 5-HT (EC_{50} ~22 nM), relatively fast on kinetics (τ_{on} ~ 70 ms), high specificity and spatial resolution and a minimal impact on cellular physiology and thus is well suited for detecting physiologically relevant endogenous 5-HT release. Indeed, we demonstrated the utility of the $GRAB_{5\text{-}HT1.0}$ sensor in detecting endogenous 5-HT release in response to a variety of stimuli and under various behavioral conditions in different animal models. Our finding that 5-HT levels change dynamically throughout the sleep–wake cycle in mice provides new insights into the functional contribution of 5-HT to sleep regulation.

Regarding potential buffering by the 5-HT1.0 sensor, we measured G protein coupling by exogenously applying 5-HT at a broad range of concentrations in the 5-HT2C and 5-HT2C with 5-HT1.0 groups in cultured cells and did not observe a significant difference in 5-HT2C receptor-mediated G protein signaling between these two groups. In addition, the *Drosophila* in vivo imaging data also showed that the expression of 5-HT1.0 has little effect on odor-evoked neuronal calcium signals. Nevertheless, one still needs to be mindful about the buffering effect of the 5-HT1.0 sensor, especially under conditions of very low local 5-HT concentrations or very high 5-HT1.0 expression levels. One way to ameliorate the buffering effect is to balance expression levels and the photons (signal) generated from the 5-HT1.0 sensor. Future efforts could be applied to tune the sensor's affinity while improving its brightness and $\Delta F/F_0$.

Of note, there is a tradeoff between a sensor's affinity and off kinetics. Given the high affinity of the 5-HT1.0 sensor, it inevitably shows slightly slow off kinetics. These kinetic features could be beneficial, as the rapid on kinetics precisely reports the initial timing of endogenous 5-HT release (for example, in local synaptic transmission), while the slow off kinetics helps to accumulate more photons and contributes to the high SNR. Nevertheless, fully capturing the dynamics of fast endogenous serotonergic signaling awaits future improvement of better sensors with both fast on and off kinetics.

Online content

Any methods, additional references, Nature Research reporting summaries, source data, extended data, supplementary information, acknowledgements, peer review information; details of author contributions and competing interests; and statements of data and code availability are available at https://doi.org/10.1038/s41593-021-00823-7.

Received: 23 February 2020; Accepted: 19 February 2021;
Published online: 05 April 2021

References

1. Lesch, K. P. et al. Association of anxiety-related traits with a polymorphism in the serotonin transporter gene regulatory region. *Science* **274**, 1527–1531 (1996).
2. Li, Y. et al. Serotonin neurons in the dorsal raphe nucleus encode reward signals. *Nat. Commun.* **7**, 10503 (2016).
3. Portas, C. M. et al. On-line detection of extracellular levels of serotonin in dorsal raphe nucleus and frontal cortex over the sleep/wake cycle in the freely moving rat. *Neuroscience* **83**, 807–814 (1998).
4. Vaswani, M., Linda, F. K. & Ramesh, S. Role of selective serotonin reuptake inhibitors in psychiatric disorders: a comprehensive review. *Prog. Neuropsychopharmacol. Biol. Psychiatry* **27**, 85–102 (2003).
5. Fuller, R. W. Uptake inhibitors increase extracellular serotonin concentration measured by brain microdialysis. *Life Sci.* **55**, 163–167 (1994).
6. Bunin, M. A., Prioleau, C., Mailman, R. B. & Wightman, R. M. Release and uptake rates of 5-hydroxytryptamine in the dorsal raphe and substantia nigra reticulata of the rat brain. *J. Neurochem.* **70**, 1077–1087 (1998).
7. Candelario, J. & Chachisvilis, M. Mechanical stress stimulates conformational changes in 5-hydroxytryptamine receptor 1B in bone cells. *Cell. Mol. Bioeng.* **5**, 277–286 (2012).
8. Jing, M. et al. A genetically encoded fluorescent acetylcholine indicator for in vitro and in vivo studies. *Nat. Biotechnol.* **36**, 726–737 (2018).
9. Patriarchi, T. et al. Ultrafast neuronal imaging of dopamine dynamics with designed genetically encoded sensors. *Science* **360**, eaat4422 (2018).
10. Sun, F. et al. A genetically encoded fluorescent sensor enables rapid and specific detection of dopamine in flies, fish, and mice. *Cell* **174**, 481–496 (2018).
11. Feng, J. et al. A genetically encoded fluorescent sensor for rapid and specific in vivo detection of norepinephrine. *Neuron* **102**, 745–761 (2019).
12. Bajar, B. T. et al. Improving brightness and photostability of green and red fluorescent proteins for live cell imaging and FRET reporting. *Sci. Rep.* **6**, 20889 (2016).
13. Pedelacq, J. D., Cabantous, S., Tran, T., Terwilliger, T. C. & Waldo, G. S. Engineering and characterization of a superfolder green fluorescent protein. *Nat. Biotechnol.* **24**, 79–88 (2006).
14. Peng, Y. et al. 5-HT2C receptor structures reveal the structural basis of GPCR polypharmacology. *Cell* **172**, 719–730 (2018).
15. Ballesteros, J. A. & Weinstein, H. [19] Integrated methods for the construction of three-dimensional models and computational probing of structure-function relations in G protein-coupled receptors. *Methods in Neurosciences* **25**, 366–428 (1995).
16. Harada, K. et al. Red fluorescent protein-based cAMP indicator applicable to optogenetics and in vivo imaging. *Sci. Rep.* **7**, 7351 (2017).
17. Wan, Q. et al. Mini G protein probes for active G protein-coupled receptors (GPCRs) in live cells. *J. Biol. Chem.* **293**, 7466–7473 (2018).
18. Barnea, G. et al. The genetic design of signaling cascades to record receptor activation. *Proc. Natl Acad. Sci. USA* **105**, 64–69 (2008).
19. Ishimura, K. et al. Quantitative analysis of the distribution of serotonin-immunoreactive cell bodies in the mouse brain. *Neurosci. Lett.* **91**, 265–270 (1988).

20. Waddell, S., Armstrong, J. D., Kitamoto, T., Kaiser, K. & Quinn, W. G. The amnesiac gene product is expressed in two neurons in the *Drosophila* brain that are critical for memory. *Cell* **103**, 805–813 (2000).
21. Lee, P. T. et al. Serotonin–mushroom body circuit modulating the formation of anesthesia-resistant memory in *Drosophila*. *Proc. Natl Acad. Sci. USA* **108**, 13794–13799 (2011).
22. Keene, A. C. et al. Diverse odor-conditioned memories require uniquely timed dorsal paired medial neuron output. *Neuron* **44**, 521–533 (2004).
23. Yu, D. et al. *Drosophila* DPM neurons form a delayed and branch-specific memory trace after olfactory classical conditioning. *Cell* **123**, 945–957 (2005).
24. Xu, M. et al. Basal forebrain circuit for sleep–wake control. *Nat. Neurosci.* **18**, 1641–1647 (2015).
25. Ren, J. et al. Anatomically defined and functionally distinct dorsal raphe serotonin sub-systems. *Cell* **175**, 472–487 (2018).
26. Oikonomou, G. et al. The serotonergic raphe promote sleep in zebrafish and mice. *Neuron* **103**, 686–701 (2019).
27. Ren, J. et al. Single-cell transcriptomes and whole-brain projections of serotonin neurons in the mouse dorsal and median raphe nuclei. *eLife* **8**, e49424 (2019).
28. Rudnick, G. & Wall, S. C. The molecular mechanism of 'ecstasy' [3,4-me thylenedioxy-methamphetamine (MDMA)]: serotonin transporters are targets for MDMA-induced serotonin release. *Proc. Natl Acad. Sci. USA* **89**, 1817–1821 (1992).
29. Bicks, L. K., Koike, H., Akbarian, S. & Morishita, H. Prefrontal cortex and social cognition in mouse and man. *Front. Psychol.* **6**, 1805 (2015).
30. Liechti, M. E., Saur, M. R., Gamma, A., Hell, D. & Vollenweider, F. X. Psychological and physiological effects of MDMA ('ecstasy') after pretreatment with the 5-HT2 antagonist ketanserin in healthy humans. *Neuropsychopharmacology* **23**, 396–404 (2000).
31. Hagino, Y. et al. Effects of MDMA on extracellular dopamine and serotonin levels in mice lacking dopamine and/or serotonin transporters. *Curr. Neuropharmacol.* **9**, 91–95 (2011).
32. Wang, Q., Shui, B., Kotlikoff, M. I. & Sondermann, H. Structural basis for calcium sensing by GCaMP2. *Structure* **16**, 1817–1827 (2008).

Methods

Primary cultures. Male and female postnatal day (P)0 Sprague–Dawley rat pups were obtained from Beijing Vital River and were used to prepare cortical neurons. The cortex was dissected, and neurons were dissociated using 0.25% trypsin–EDTA (Gibco), plated on 12-mm glass coverslips coated with poly-D-lysine (Sigma-Aldrich) and cultured in neurobasal medium (Gibco) containing 2% B-27 supplement (Gibco), 1% GlutaMAX (Gibco) and 1% penicillin–streptomycin (Gibco). Neurons were cultured at 37 °C in a humidified atmosphere in air containing 5% CO_2.

Cell lines. HEK293T cells were purchased from ATCC and verified based on their morphology observed by microscopy and an analysis of their growth curve. Stable cell lines expressing either the 5-HT2C receptor or 5-HT1.0 were generated by cotransfecting cells with the PiggyBac plasmid carrying the target genes together with that encoding Tn5 transposase into a stable HEK293T cell line. Cells expressing the target genes were selected using 2 μg ml^{-1} puromycin (Sigma). An HEK293T cell line stably expressing a tTA-dependent luciferase reporter and the gene encoding the β-arrestin2–TEV fusion used in the Tango assay was a generous gift from B.L. Roth (University of North Carolina Chapel Hill Medical School)[33]. All cell lines were cultured at 37 °C with 5% CO_2 in DMEM (Gibco) supplemented with 10% (vol/vol) FBS (Gibco) and 1% penicillin–streptomycin (Gibco).

Drosophila. UAS-GRAB$_{5\text{-}HT1.0}$ (attp40, UAS-GRAB$_{5\text{-}HT1.0}$/CyO) and UAS-GRAB$_{5\text{-}HTmut}$ (attp40, UAS-GRAB$_{5\text{-}HTmut}$/CyO) flies were generated in this study. The coding sequences of GRAB$_{5\text{-}HT1.0}$ or that of GRAB$_{5\text{-}HTmut}$ was inserted into pJFRC28 (ref. [34]) (Addgene plasmid 36431) using Gibson assembly. These vectors were injected into embryos and integrated into attp40 via phiC31 by the Core Facility of Drosophila Resource and Technology, Shanghai Institute of Biochemistry and Cell Biology, Chinese Academy of Sciences. The following fly stocks were used in this study: R13F02-Gal4 (BDSC, 48571), VT64246-Gal4 (VDRC, 204311) and UAS-jRCaMP1a (BDSC, 63792)[35]. Flies were raised on standard cornmeal–yeast medium at 25 °C, with 70% relative humidity and a 12-h–12-h light–dark cycle. In Fig. 2h–j and Extended Data Fig. 6a–c, UAS-GRAB$_{5\text{-}HT1.0}$/CyO;R13F02-Gal4/TM2 flies were used; in Fig. 2k,l, UAS-CsChrimson-mCherry/CyO;VT64246-Gal4/TM2 flies were used; in Fig. 2m–q, UAS-GRAB$_{5\text{-}HT1.0}$/CyO;VT64246-Gal4/TM2 flies were used; in Fig. 2r–t and Extended Data Fig. 6j,k, UAS-GRAB$_{5\text{-}HT1.0}$/+;R13F02-Gal4/UAS-jRCaMP1a and R13F02-Gal4/UAS-jRCaMP1a flies were used; in Extended Data Fig. 6d–i, UAS-GRAB$_{5\text{-}HT1.0}$/CyO;R13F02-Gal4/TM2 and UAS-GRAB$_{5\text{-}HTmut}$/+;R13F02-Gal4/+ flies were used.

Mice. Wild-type male and female C57BL/6 (P25–P60) mice were used to prepare acute brain slices and for in vivo mouse experiments. All mice were group housed in a temperature-controlled room (21.5 °C) with a 12-h–12-h light–dark cycle with humidity controlled at 55% and were provided with food and water ad libitum. All procedures for animal surgery and maintenance were performed using protocols that were approved by the Animal Care and Use Committees at Peking University, the Chinese Academy of Sciences and the University of Virginia and were performed following the guidelines established by the US National Institutes of Health (NIH).

Molecular biology. Plasmids were generated using the Gibson assembly method[36], and DNA fragments were amplified by PCR using primers (Thermo Fisher Scientific) with an overlap of 25–30 bp. DNA fragments were assembled using T5 exonuclease (New England Biolabs), Phusion DNA polymerase (Thermo Fisher Scientific) and Taq ligase (iCloning). Sanger sequencing was performed at the Sequencing Platform in the School of Life Sciences at Peking University to verify plasmid sequences. cDNA encoding various 5-HT receptors (HTR1E, HTR2C, HTR5A and HTR6) was generated by PCR amplification of the full-length human GPCR cDNA library (hORFeome database 8.1). For optimizing the 5-HT sensor, cDNA encoding the candidates in steps 1 and 2 was cloned into the pDisplay vector (Invitrogen) with an IgK leader sequence upstream of the region coding for the sensor. In step 3, in addition to the upstream IgK peptide, DNA for the IRES-mCherry-CAAX cascade was fused downstream of that for the sensor to calibrate the membrane signal. For optimizing the linker sequence and cpGFP, site-directed mutagenesis was performed using primers containing NNB codons (48 codons, encoding 20 possible amino acids). For characterization in cultured rat cortical neurons, DNA encoding GRAB$_{5\text{-}HT1.0}$ and GRAB$_{5\text{-}HTmut}$ was cloned into the pAAV vector under the *hSyn*, *TRE* or *CAG* promoter. In downstream coupling experiments, DNA encoding the GRAB$_{5\text{-}HT}$ sensor and the 5-HT2C receptor were cloned into the pTango and pPiggyBac vectors, respectively. Two mutations were introduced into pCS7-PiggyBAC to generate hyperactive piggyBac transposase (ViewSolid Biotech)[37]. The GRAB$_{5\text{-}HT1.0}$-SmBit and 5-HT2C-SmBit constructs were derived from β2AR-SmBit[17] using a BamHI site incorporated upstream of DNA encoding the GGSG linker. LgBit-mGq was a generous gift from N.A. Lambert (Augusta University).

Expression of GRAB$_{5\text{-}HT}$ in cultured cells and in vivo. HEK293T cells were plated on 12-mm glass coverslips in 24-well plates and grown to 70% confluence for transfection with PEI (1 μg DNA and 3 μg PEI per well), the medium was replaced after 4–6 h, and cells were used for imaging 24 h after transfection. Cultured rat cortical neurons were infected with AAVs expressing *TRE*-GRAB$_{5\text{-}HT1.0}$ (titer, 3.8×10^{13} particles per ml) and *hSyn*-tTA (titer, 1.3×10^{14} particles per ml) or *hSyn*-GRAB$_{5\text{-}HTmut}$ (titer, 1×10^{13} particles per ml) after 7–9 d of in vitro culture, and imaging was performed 7–14 d after infection.

For in vivo expression, mice were deeply anesthetized with an i.p. injection of 2,2,2-tribromoethanol (Avertin, 500 mg per kg, Sigma-Aldrich) or ketamine (10 mg per kg) and xylazine (2 mg per kg) and placed in a stereotaxic frame, and AAVs were injected using a microsyringe pump (Nanoliter 2000 Injector, WPI). For the experiments shown in Extended Data Fig. 5a–d, AAV expressing *hSyn*-GRAB$_{5\text{-}HT1.0}$ (titer, 4.6×10^{13} particles per ml) was injected (volume, 400 nl) into the hippocampus at the following coordinates relative to the bregma: anterior–posterior (AP), −2.0 mm; medial–lateral (ML), 1.5 mm (depth, 2.3 mm). For the experiments shown in Fig. 2a–e and Extended Data Fig. 5e–h, AAVs expressing *CAG*-GRAB$_{5\text{-}HT1.0}$ (titer, 1.3×10^{13} particles per ml) or *hSyn*-GRAB$_{5\text{-}HTmut}$ (titer, 1×10^{13} particles per ml) were injected (volume, 400 nl) into the DRN at the following coordinates relative to the bregma: AP, −4.3 mm; ML, 1.1 mm (depth, 2.85 mm, with a 20° ML angle). For the experiments shown in Fig. 2f,g and Extended Data Fig. 5i,j, Sindbis virus expressing GRAB$_{5\text{-}HT1.0}$ was injected (volume, 50 nl) into the DRN at the following coordinates relative to the bregma: AP, −4.3 mm; ML, 0.0 mm (depth, 3.00 mm). For the experiments shown in Fig. 3a–g, AAVs expressing *CAG*-GRAB$_{5\text{-}HT1.0}$ or *hSyn*-GRAB$_{5\text{-}HTmut}$ were injected (volume, 400 nl) into the BF at the following coordinates relative to the bregma: AP, 0 mm; ML, 1.3 mm (depth, 5.0 mm), the OFC (AP, +2.6 mm; ML, 1.7 mm (depth, 1.7 mm)) and the BNST (AP, +0.14 mm; ML, 0.8 mm (depth, 3.85 mm)). For the experiments shown in Fig. 3h–k, AAVs expressing *hSyn*-GRAB$_{5\text{-}HT1.0}$ (titer, 4.6×10^{13} particles per ml) or *hSyn*-GRAB$_{5\text{-}HTmut}$ (titer, 1×10^{13} particles per ml) were injected (volume, 400 nl) into the PFC at the following coordinates relative to the bregma: AP, +2.8 mm; ML, 0.5 mm (depth, 0.5 mm).

Fluorescence imaging of HEK293T cells and cultured rat cortical neurons. An inverted Ti-E A1 confocal microscope (Nikon) and an Opera Phenix high-content screening system (PerkinElmer) were used for imaging. The confocal microscope was equipped with a ×40, 1.35-numerical aperture (NA), oil-immersion objective, a 488-nm laser and a 561-nm laser. The GFP signal was collected using a 525/50-nm emission filter, and the RFP signal was collected using a 595/50-nm emission filter. Cultured cells expressing GRAB$_{5\text{-}HT1.0}$ or GRAB$_{5\text{-}HTmut}$ were either bathed or perfused with Tyrode's solution containing (in mM) 150 NaCl, 4 KCl, 2 $MgCl_2$, 2 $CaCl_2$, 10 HEPES and 10 glucose (pH 7.4). Drugs were delivered via a custom-made perfusion system or by bath application. The chamber was cleaned thoroughly between experiments using 75% ethanol. Photostability was measured using confocal microscopy (one-photon illumination) with the 488-nm laser at a laser power of 350 μW, and the Opera Phenix high-content screening system was equipped with a ×40, 1.1-NA water-immersion objective, a 488-nm laser and a 561-nm laser; the GFP signal was collected using a 525/50-nm emission filter, and the RFP signal was collected with a 600/30-nm emission filter. For imaging, the culture medium was replaced with 100 μl Tyrode's solution, and drugs (at various concentrations) were applied in Tyrode's solution. The fluorescence signal of the GRAB$_{5\text{-}HT}$ sensors was calibrated using the GFP:RFP ratio. To measure the response kinetics of the 5-HT1.0 sensor, the line-scanning mode of the confocal was used to record rapid changes in fluorescence. A glass pipette filled with 10 μM 5-HT or Met was placed near 5-HT1.0 sensor-expressing HEK293T cells. Met or 5-HT was puffed from the pipette to measure the off and on response kinetics, respectively. For calculating the on and off kinetics, different F_0 values were used. In detail, we used the basal fluorescent intensity before 5-HT applications as F_0 when calculating the 'on' response, while when calculating the 'off' response, we used the fluorescence intensity of 5-HT1.0 under saturating 5-HT conditions (10 μM) as F_0.

Tango assay. First, 5-HT at various concentrations was applied to 5-HT2C-expressing or 5-HT1.0-expressing HTLA cells[33]. The cells were then cultured for 12 h to allow expression of firefly luciferase. Bright-Glo reagent (Fluc Luciferase Assay System, Promega) was then added at a final concentration of 5 μM, and luminescence was measured using a Victor X5 multilabel plate reader (PerkinElmer).

Luciferase complementation assay. The luciferase complementation assay was performed as previously described[17]. In brief, 48 h after transfection, cells were washed with PBS, collected by trituration and transferred to opaque 96-well plates containing 5-HT at various concentrations. Furimazine (NanoLuc Luciferase Assay, Promega) was then added quickly to each well, followed by measurement with Nluc.

Fluorescence imaging of GRAB$_{5\text{-}HT}$ in mouse brain slices. AAVs or Sindbis virus expressing GRAB$_{5\text{-}HT1.0}$ or GRAB$_{5\text{-}HTmut}$ were injected into the mouse hippocampus or the DRN as described above. Three weeks after AAV injection or 18 h after Sindbis virus injection, mice were deeply anesthetized with an i.p. injection of Avertin or xylazine–ketamine and then transcardially perfused with 10 ml oxygenated slicing buffer consisting of (in mM) 110 choline-Cl, 2.5 KCl, 1 NaH_2PO_4, 25

$NaHCO_3$, 7 $MgCl_2$, 25 glucose and 0.5 $CaCl_2$. Mice were then decapitated, and brains were removed and placed in cold (0–4 °C) oxygenated slicing buffer for an additional 1 min. Next, brains were rapidly mounted on the cutting stage of a VT1200 vibratome (Leica) for coronal sectioning at a thickness of 300 µm. Brain slices containing the hippocampus or the DRN were initially allowed to recover for ≥40 min at 34 °C in oxygen-saturated Ringer's buffer consisting of (in mM) 125 NaCl, 2.5 KCl, 1 NaH_2PO_4, 25 $NaHCO_3$, 1.3 $MgCl_2$, 25 glucose and 2 $CaCl_2$. For two-photon imaging, slices were transferred to a recording chamber that was continuously perfused with oxygen-saturated Ringer's buffer at 34 °C and placed in an FV1000MPE two-photon microscope (Olympus) equipped with a ×25, 1.05-NA water-immersion objective. Next, 5-HT1.0 or 5-HTmut fluorescence was excited using a mode-locked Mai Tai Ti:Sapphire laser (Spectra-Physics) at a wavelength of 920 nm and collected with a 495–540-nm filter. For electrical stimulation, a bipolar electrode (WE30031.0A3, MicroProbes) was positioned near the DRN in the slice, and imaging and stimulation were synchronized using an Arduino board with a custom-written program. The parameters of the frame scan were set to a size of 128 × 96 pixels with a speed of 0.1482 s per frame for electrical stimulation and a size of 512 × 512 pixels with a speed of 1.109 s per frame for drug perfusion experiments. For kinetics measurements, line scans were performed at a rate of 800–850 Hz. The stimulation voltage was set at 4–6 V, and the duration of each stimulation was set at 1 ms. Drugs were bath applied by perfusion into the recording chamber in premixed Ringer's buffer. For mouse brain slices infected with Sindbis virus, wide-field epifluorescence imaging was performed using the Hamamatsu ORCA-Flash4.0 camera (Hamamatsu Photonics), and 5-HT1.0-expressing cells in acutely prepared brain slices were excited with a 460-nm ultrahigh-power low-noise LED (Prizmatix). The frame rate of the Flash4.0 camera was set to 10 Hz. To synchronize image capture with electrical stimulation and FSCV, the camera was set to external trigger mode and triggered with a custom-written IGOR Pro 6 program (WaveMetrics). For electrical stimulation, a home-made bipolar electrode was positioned near the DRN in the slice, and the stimulation current was set at 350 µA, and the duration of each stimulation was set at 1 ms.

Fast-scan cyclic voltammetry. CFMEs were fabricated as described previously[38]. Briefly, cylindrical CFMEs (7 µm in radius) were constructed with T-650 carbon fiber (Cytec Engineered Materials), which was aspirated into a glass capillary (1.2-mm OD and 0.68-mm ID, A-M Systems), and the capillary was pulled using the PE-22 puller (Narishige International). The carbon fiber was trimmed to 50–70 µm in length from the pulled glass tip and sealed with Epon epoxy, which was cured at 100 °C for 2 h followed by incubation at 150 °C overnight. CFMEs were cleaned in isopropyl alcohol for 30 min before Nafion electrodeposition. Nafion was electrochemically deposited by submerging CFME tips in Nafion solution (5% (wt) 1100 EW Nafion in methanol, Ion Power), and a constant potential of 1.0 V versus Ag–AgCl was applied to the electrode for 30 s. Next, Nafion-coated electrodes were air dried for 10 s and then incubated at 70 °C for 10 min. For electrochemical detection of 5-HT, a Jackson waveform was applied to the electrode by scanning the potential from 0.2 V to 1.0 V to −0.1 V and back to 0.2 V at 1,000 V s^{-1} using a Chem-Clamp potentiostat (Dagan). For data collection and analysis, TarHeel CV (provided by R.M. Wightman, University of North Carolina) was used. For electrode calibration, PBS solution was used, which consisting of (in mM) 131.25 NaCl, 3.0 KCl, 10.0 NaH_2PO_4, 1.2 $MgCl_2$, 2.0 Na_2SO_4 and 1.2 $CaCl_2$ (pH 7.4). A stock solution of 5-HT was prepared in 0.1 M $HClO_4$ and diluted to 500 nM with PBS for calibrations before the experiment.

Fluorescence imaging of transgenic flies. Fluorescence imaging in flies was performed using an Olympus two-photon microscope (FV1000) equipped with a Spectra-Physics Mai Tai Ti:Sapphire laser. A 930-nm excitation laser was used for one-color imaging of 5-HT1.0 and 5-HTmut, and a 950-nm excitation laser was used for two-color imaging with 5-HT1.0 and jRCaMP1a. For detection, a 495–540-nm filter was used for the green channel, and a 575–630-nm filter was used for the red channel. Adults male flies were used for imaging within 2 weeks after eclosion. To prepare the fly for imaging, adhesive tape was affixed to the head and wings. The tape above the head was excised, and the chitin head-shell, air sacs and fat bodies were carefully removed to expose the central brain. The brain was bathed continuously in an adult hemolymph-like solution composed of (in mM) 108 NaCl, 5 KCl, 5 HEPES, 5 trehalose, 5 sucrose, 26 $NaHCO_3$, 1 NaH_2PO_4, 2 $CaCl_2$ and 1–2 $MgCl_2$. For electrical stimulation, a glass electrode (resistance, 0.2 MΩ) was placed in proximity to the MB medial lobe, and voltage for stimulation was set to 10–30 V. For odorant stimulation, the odorant isoamyl acetate (306967, Sigma-Aldrich) was first diluted 200-fold in mineral oil and then diluted fivefold with air and delivered to the antenna at a rate of 1,000 ml min^{-1}. For body shock, two copper wires were attached to the fly's abdomen, and a 500-ms electrical stimulus was delivered at 50–80 V. For 5-HT application, the blood–brain barrier was carefully removed, and 5-HT was applied at a final concentration of 100 µM. An Arduino board was used to synchronize the imaging and stimulation protocols. The sampling rates during electrical stimulation, odorant stimulation, body-shock stimulation and 5-HT perfusion were 12 Hz, 6.8 Hz, 6.8 Hz and 1 Hz, respectively.

Immunostaining in transgenic flies. For immunofluorescence, adult flies (UAS-CsChrimson-mCherry/CyO and VT64246-Gal4/TM2 flies) were dissected in PBS within 5–12 d and then subject to fixation in 4% PFA on ice for 1–4 h. Brains were washed with washing buffer (3% NaCl, 1% Triton X-100 in PBS) three times for 10 min each. Samples were transferred to penetration–blocking buffer (2% Triton X-100, 10% normal goat serum in PBS) for 20 h at 4 °C on a shaker. Samples were then transferred into a solution with primary antibody diluted with dilution buffer (0.25% Triton X-100, 1% normal goat serum in PBS) for 24 h at 4 °C. After washing three times, samples were incubated with the secondary antibody for 14–20 h at 4 °C on the shaker. Lastly, samples were washed three times and mounted with 50% glycerol. The primary and secondary antibodies were rabbit anti-mCherry (1:500, Abcam, ab167453; RRID, AB_2571870) and Alex Fluor 647 goat anti-rabbit (1:500, AAT Bioquest, 16710). An inverted Ti-E A1 confocal microscope (Nikon) was used for immunofluorescence imaging. The confocal microscope was equipped with a ×20, 0.75-NA air objective. A 640-nm laser and a 663/738-nm emission filter were used for this experiment.

Two-photon imaging in mice. Fluorescence imaging in mice was performed using an Olympus two-photon microscope (FV1000) equipped with a Spectra-Physics Mai Tai Ti:Sapphire laser. The excitation wavelength was 920 nm, and fluorescence was collected using a 495–540-nm filter. To perform imaging in head-fixed mice, part of the mouse scalp was removed, and the underlying tissues and muscles were carefully removed to expose the skull. A metal recording chamber was affixed to the skull surface with glue, followed by a thin layer of dental cement to strengthen the connection. One to two days later, the skull above the PFC was carefully removed, taking care to avoid major blood vessels. AAVs expressing $GRAB_{5\text{-}HT1.0}$ or $GRAB_{5\text{-}HTmut}$ were injected as described above. A custom-made 4 mm × 4 mm square coverslip was placed over the exposed PFC and secured with glue. After surgery, mice were allowed to recover for at least 3 weeks. Mice were then fixed to the base and allowed to habituate for 2–3 d. During the experiment, drugs were administered by i.p. injection, and the sampling rate was 0.1 Hz.

Fiber-photometry recording in mice. To monitor 5-HT release in various brain regions during the sleep–wake cycle, AAVs expressing $GRAB_{5\text{-}HT1.0}$ or $GRAB_{5\text{-}HTmut}$ were injected via a glass pipette into the BF, OFC and BNST using a Nanoject II (Drummond Scientific). An optical fiber (200 µm, 0.37 NA) with FC ferrule was carefully inserted at the same coordinates used for virus injection. The fiber was affixed to the skull surface using dental cement. After surgery, mice were allowed to recover for at least 1 week. The photometry rig was constructed using parts obtained from Doric Lenses, including a fluorescence optical mini cube (FMC4_AE(405)_E(460–490)_F(500–550)_S), a blue LED (CLED_465), an LED driver (LED_2) and a photoreceiver (NPM_2151_FOA_FC). To record $GRAB_{5\text{-}HT1.0}$ and $GRAB_{5\text{-}HTmut}$ fluorescence signals, a beam of excitation light was emitted from an LED at 20 µW, and the optical signals from $GRAB_{5\text{-}HT1.0}$ and $GRAB_{5\text{-}HTmut}$ were collected through optical fibers. For fiber-photometry data, a software-controlled lock-in detection algorithm was implemented in the TDT RZ2 system using the fiber-photometry 'Gizmo' in the Synapse software program (modulation frequency, 459 Hz; low-pass filter for demodulated signal, 20 Hz, sixth order). Photometry data were collected with a sampling frequency of 1,017 Hz. The recording fiber was bleached before recording to eliminate autofluorescence from the fiber, and the background fluorescence intensity was recorded and subtracted from the recorded signal during data analysis.

Electroencephalography and electromyography recordings. Mice were anesthetized with isoflurane (5% for induction; 1.5–2% for maintenance) and placed on a stereotaxic frame with a heating pad. For EEG, two stainless steel miniature screws were inserted in the skull above the visual cortex, and two additional steel screws were inserted in the skull above the frontal cortex. For EMG, two insulated EMG electrodes were inserted in the neck musculature, and a reference electrode was attached to a screw inserted in the skull above the cerebellum. The screws in the skull were affixed using thick dental cement. All experiments were performed at least 1 week after surgery. TDT system 3 amplifiers (RZ2 and PZ5) were used to record EEG and EMG signals; the signal was passed through a 0.5-Hz high-pass filter and digitized at 1,526 Hz.

Quantification and statistical analysis. Animals or cells were randomly assigned into control or experimental groups. Data collection and analysis were not performed blind to the conditions of the experiments, and no data were excluded for the analysis. No statistical methods were used to predetermine sample sizes, but our sample sizes are similar to those reported in previous publications[8–11]. Imaging data from cultured HEK293T cells, cultured rat cortical neurons, acute mouse brain slices, transgenic flies and head-fixed mice were processed using ImageJ (1.52p) software (NIH) and analyzed using custom-written MATLAB (R2020a) programs. Traces were plotted using Origin 2020 (2020b). Exponential-function fitting in Origin was used to correct for slight photobleaching of the traces in Fig. 2i,n–p,r,s and Extended Data Fig. 6c,f–h. In Fig. 2n–p and Extended Data Fig. 6b,e, background levels measured outside the region of interest of the pseudocolor images were removed using ImageJ. Imaging data from head-fixed mice were corrected a using motion-correction algorithm (EZcalcium) to correct movement artifacts[39].

For fiber-photometry data analysis, raw data were binned into 1-Hz bins (that is, downsampled by 1,000), and background autofluorescence was

subtracted. For calculating $\Delta F/F_0$, a baseline value was obtained by fitting the autofluorescence-subtracted data with a second-order exponential function. Slow drift was removed from the z-score-transformed $\Delta F/F_0$ values using the MATLAB script 'BEADS' with a cutoff frequency of 0.00035 cycles per sample (https://www.mathworks.com/matlabcentral/fileexchange/49974-beads-baseline-estimation-and-denoising-with-sparsity). To quantify the change in 5-HT fluorescence across multiple animals, the z-score-transformed $\Delta F/F_0$ values were further normalized using the standard deviation of the signal measured during REM sleep (when there was no apparent fluctuation in the signal), yielding a normalized z score. This normalized z score was used for the analysis in Fig. 3a–g.

For EEG and EMG data analysis, fast Fourier transform was used to perform spectral analysis with a frequency resolution of 0.18 Hz. The brain state was classified semi-automatically in 5-s epochs using a MATLAB GUI and then validated manually by trained experimenters. Wakefulness was defined as desynchronized EEG activity combined with high EMG activity, and NREM sleep was defined as synchronized EEG activity combined high-amplitude delta activity (0.5–4 Hz) combined with low EMG activity, and REM sleep was defined as high power at theta frequencies (6–9 Hz) combined with low EMG activity.

Except when indicated otherwise, all summary data are reported as mean ± s.e.m. The SNR was calculated as the peak response divided by the standard deviation of the baseline fluorescence. Data distribution was assumed to be normal, and equal variances were formally tested. Two-tailed Student's t-tests and one-way ANOVA tests were performed. P values are denoted by $^*P<0.05$, $^{**}P<0.01$, $^{***}P<0.001$ and NS ($P>0.05$). Exact P values are specified in the legends. Cartoons in Fig. 3a,d,f,h were created with https://biorender.com/.

Reporting Summary. Further information on research design is available in the Nature Research Reporting Summary linked to this article.

Data availability

Plasmids for expressing the sensors used in this study were deposited at Addgene (https://www.addgene.org/140552/). The human GPCR cDNA library was obtained from the hORFeome database 8.1 (http://horfdb.dfci.harvard.edu/index.php?page=home). Source data are provided with this paper.

Code availability

The EZcalcium algorithm and BEADS baseline estimation and denoising with sparsity algorithm are available at https://github.com/porteralab/EZcalcium and https://www.mathworks.com/matlabcentral/fileexchange/49974-beads-baseline-estimation-and-denoising-with-sparsity.

References

33. Kroeze, W. K. et al. PRESTO-Tango as an open-source resource for interrogation of the druggable human GPCRome. *Nat. Struct. Mol. Biol.* **22**, 362–369 (2015).
34. Pfeiffer, B. D., Truman, J. W. & Rubin, G. M. Using translational enhancers to increase transgene expression in *Drosophila*. *Proc. Natl Acad. Sci. USA* **109**, 6626–6631 (2012).
35. Dana, H. et al. Sensitive red protein calcium indicators for imaging neural activity. *eLife* **5**, e12727 (2016).
36. Gibson, D. G. et al. Enzymatic assembly of DNA molecules up to several hundred kilobases. *Nat. Methods* **6**, 343–345 (2009).
37. Yusa, K. et al. Targeted gene correction of α1-antitrypsin deficiency in induced pluripotent stem cells. *Nature* **478**, 391–394 (2011).
38. Shin, M. & Venton, B. J. Electrochemical measurements of acetylcholine-stimulated dopamine release in adult *Drosophila melanogaster* brains. *Anal. Chem.* **90**, 10318–10325 (2018).
39. Cantu, D. A. et al. EZcalcium: open-source toolbox for analysis of calcium imaging data. *Front. Neural Circuits* **14**, 25 (2020).

Acknowledgements

We thank Y. Rao for providing the two-photon microscope and X. Lei at PKU-CLS and the National Center for Protein Sciences at Peking University for support and assistance with the Opera Phenix high-content screening system. We thank D. Lin and X. Xu for critical reading of the manuscript. This work was supported by the Beijing Municipal Science & Technology Commission (Z181100001318002), the Beijing Brain Initiative of the Beijing Municipal Science & Technology Commission (Z181100001518004), a Guangdong grant, 'Key Technologies for Treatment of Brain Disorders' (2018B030332001), the General Program of National Natural Science Foundation of China (projects 31671118, 31871087 and 31925017), the Science Fund for Creative Research Groups of the National Natural Science Foundation of China (81821092), the NIH BRAIN Initiative (NS103558), grants from the Peking-Tsinghua Center for Life Sciences and the State Key Laboratory of Membrane Biology at Peking University School of Life Sciences (to Y.L.), the Shanghai Municipal Science and Technology Major Project (2018SHZDZX05 to M.X.) and the Shanghai Pujiang Program (18PJ1410800 to M.X.), a Peking University Postdoctoral Fellowship (J.F.), an Alzheimer's Association Postdoctoral Research Fellowship (AARF 19 619387 to P.Z.), a Peking-Tsinghua Center Excellence Postdoctoral Fellowship (Y.Z.) and the Beijing Nova Program (Z201100006820100 to M.J.).

Author contributions

Y.L. conceived and supervised the project. J.W., M.J., F.D., S.H., J.F., J. Zou and S.P. performed the experiments related to developing, optimizing and characterizing the sensor in cultured HEK293T cells and neurons. T.Q. performed the experiments using AAVs in slices. P.Z., Y.Z. and M.S. performed the simultaneous imaging and FSCV experiments using the Sindbis virus in slices under the supervision of J.J.Z. and B.J.V. X.L. and J. Zeng performed the *Drosophila* experiments. W.P. and K.S. performed the fiber-photometry recordings in behaving mice under the supervision of M.X. J.W. performed two-photon imaging of head-fixed mice. All authors contributed to data interpretation and analysis. Y.L. and J.W. wrote the manuscript with input from all other authors.

Competing interests

The authors declare competing financial interests. J.W., M.J., J.F. and Y.L. have filed patent applications, the value of which might be affected by this publication.

Additional information

Extended data is available for this paper at https://doi.org/10.1038/s41593-021-00823-7.

Supplementary information The online version contains supplementary material available at https://doi.org/10.1038/s41593-021-00823-7.

Correspondence and requests for materials should be addressed to Y.L.

Peer review information *Nature Neuroscience* thanks Adam Cohen and the other, anonymous, reviewer(s) for their contribution to the peer review of this work.

Reprints and permissions information is available at www.nature.com/reprints.

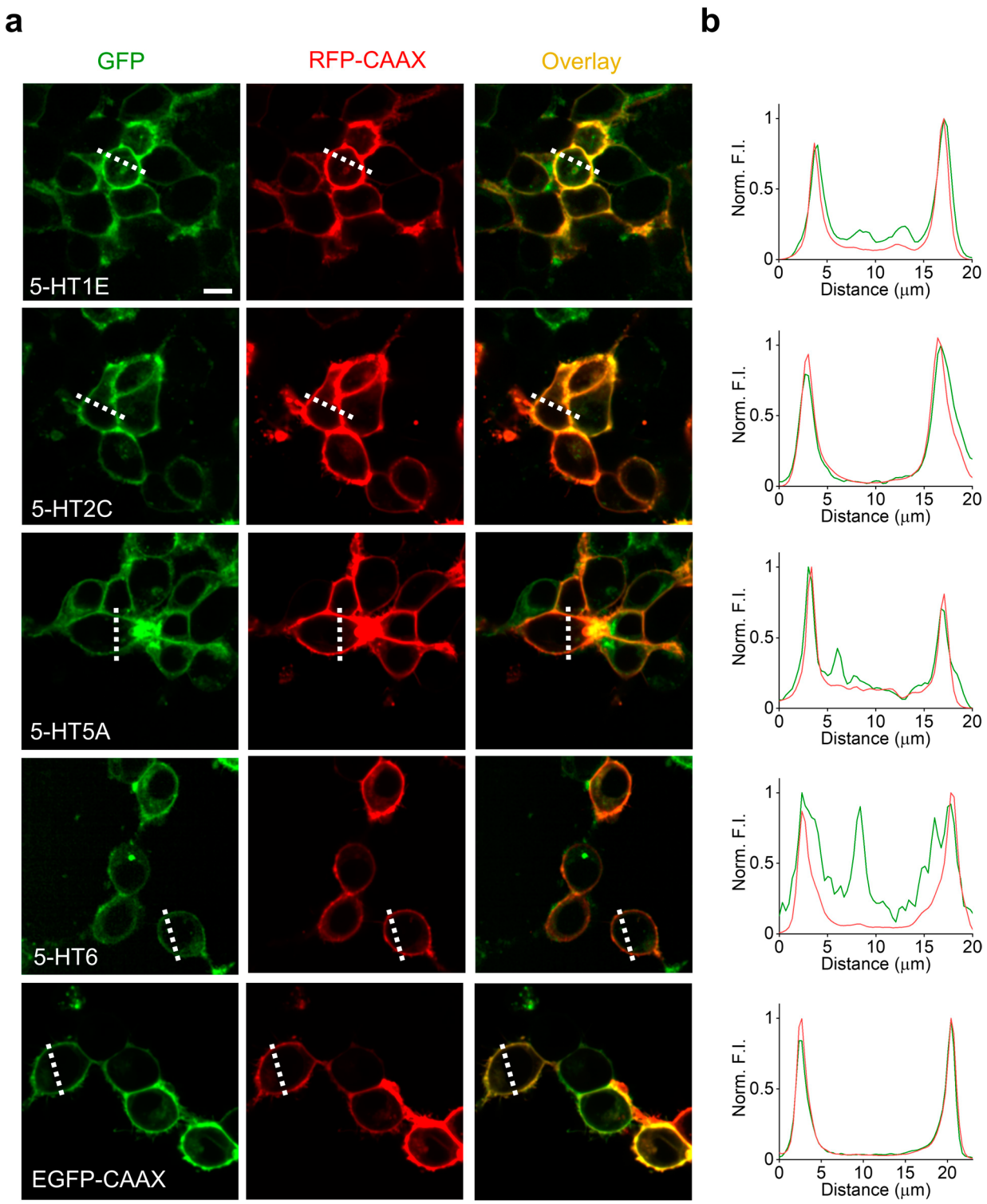

Extended Data Fig. 1 | Characterization of the membrane trafficking for 5-HT receptor-based chimeras. a, Representative fluorescence images of HEK293T cells co-expressing the indicated 5-HT receptors fused with cpGFP (green) and RFP-CAAX (red); EGFP-CAAX was used as a positive control. Similar results were observed for more than 100 cells. Scale bar, 10 μm. **b**, Normalized fluorescence intensity measured at the white dashed lines shown in (**a**) for each candidate sensor.

a

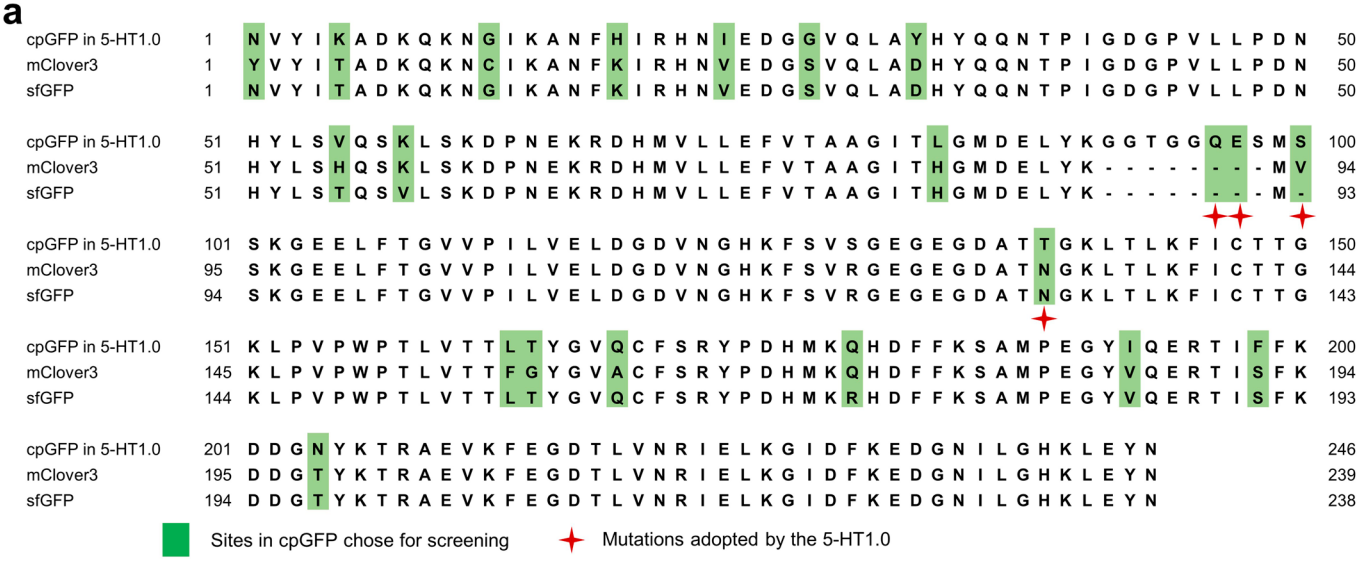

Extended Data Fig. 2 | Sequence alignment of cpGFP from 5-HT1.0 sensor, sfGFP, and mClover3. a, The sequence of cpGFP from the 5-HT1.0 sensor, sfGFP, and mClover3 are aligned. Amino acids in the cpGFP chose for optimization are labeled with light green color, and the mutations adopted by the 5-HT1.0 sensor are indicated with red stars.

a

b

```
1   METDTLLLWVLLLWVPGSTGDTSLYKKVGTTGVNLRNAVHSFLVHLIGLL  50
51  VWQCDISVSPVAAIVTDIFNTSDGGRFKFPDGVQNWPALSIVIIIIMTIG 100
101 GNILVIMAVSMEKKLHNATNYFLMSLAIADMLVGLLVMPLSLLAILYDYV 150
151 WPLPRYLCPVWISLDVLFSTASIMHLCAISLDRYVAIRNPIEHSRFNSRT 200
201 KAIMKIAIVWAISIGVSVPIPVIGLRDEEKVFVNNTTCVLNDPNFVLIGS 250
251 FVAFFIPLTIMVITYCLTIYVLRRQALMFLNGNVYIKADKQKNGIKANFH 300
301 IRHNIEDGGVQLAYHYQQNTPIGDGPVLLPDNHYLSVQSKLSKDPNEKRD 350
351 HMVLLEFVTAAGITLGMDELYKGGTGGQESMSSKGEELFTGVVPILVELD 400
401 GDVNGHKFSVSGEGEGDATTGKLTLKFICTTGKLPVPWPTLVTTLTYGVQ 450
451 CFSRYPDHMKQHDFFKSAMPEGYIQERTIFFKDDGNYKTRAEVKFEGDTL 500
501 VNRIELKGIDFKEDGNILGHKLEYNGFATANNERKASKVLGIVFFVFLIM 550
551 WCPFFITNILSVLCEKSCNQKLMEKLLNVFVWIGYVCSGINPLVYTLFNK 600
601 IYRRAFSNYLRCNYKVEKKPPVRQIPRVAATALSGRELNVNIYRHTNEPV 650
651 IEKASDNEPGIEMQVENLELPVNPSSVVSERISSV*                700
```

✦ Mutations adopted in cpGFP by the 5-HT1.0

Extended Data Fig. 3 | The amino acid sequence of 5-HT1.0. a, Schematic representation of the 5-HT1.0 structure. For simplicity, TM1-4, TM7, and H8 are not shown. **b**, The amino acid sequence of the 5-HT1.0 sensor after three steps of evolution. The mutated amino acids in cpGFP (cpGFP from GCaMP6s, see Chen, T.W., *et al*. 2013.) are indicated with red stars.

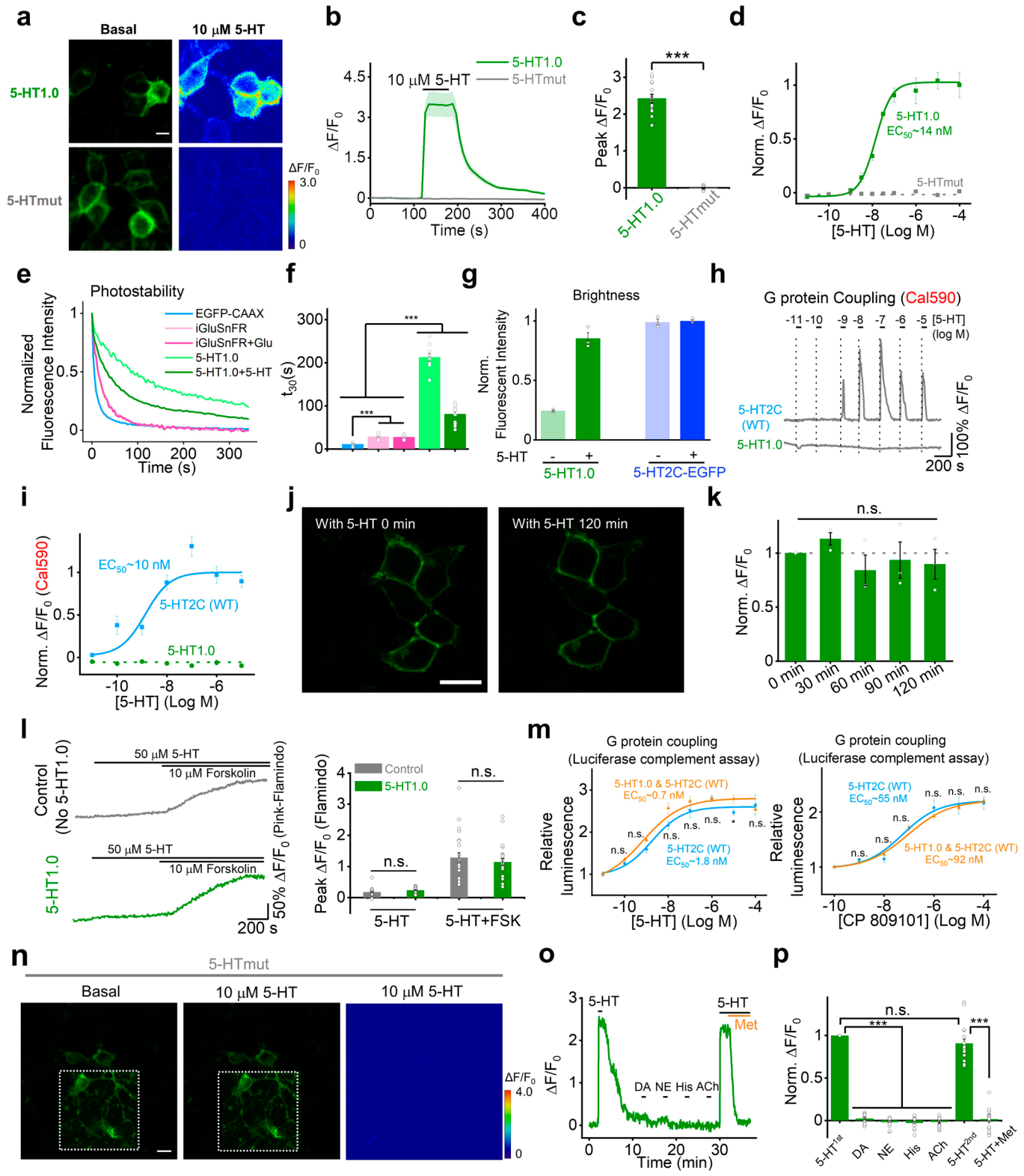

Extended Data Fig. 4 | See next page for caption.

Extended Data Fig. 4 | Further characterization of GRAB$_{5\text{-HT}}$ in cultured HEK293T cells and rat cortical neurons. a, Representative fluorescence and pseudocolor images of HEK293T cells expressing 5-HT1.0 or 5-HTmut before (left) and after (right) application of 10 μM 5-HT. Similar results were observed for more than 10 cells. Scale bar, 20 μm. **b**,**c**, Representative fluorescence traces and group summary of the peak response in HEK293T cells expressing 5-HT1.0 or 5-HTmut; n = 14 and 15 cells from 3 cultures for 5-HT1.0 and 5-HTmut group. Two-tailed Student's t-test was performed. $P = 8.18 \times 10^{-12}$ between 5-HT1.0 and 5-HTmut group. **d**, 5-HT dose-response curves measured in cells expressing 5-HT1.0 or 5-HTmut, the EC_{50} for 5-HT1.0 is shown. n = 3 wells per group with 300–500 cells per well. **e**, Representative normalized fluorescence measured in HEK293T cells expressing 5-HT1.0, EGFP-CAAX, or iGluSnFR during continuous exposure to 488-nm laser (power: 350 μW). **f**, Summary of the decay time constant calculated from the photobleaching curves shown in (**e**). n = 10/3, 14/3, and 12/3 for 5-HT1.0, EGFP-CAAX, and iGluSnFR, respectively. Two-tailed Student's t-test was performed. $P = 2.45 \times 10^{-9}$, 1.90×10^{-9}, 3.05×10^{-8}, and 7.22×10^{-7} between EGFP-CAAX and iGluSnFR without or with Glu, and 5-HT1.0 without or with 5-HT. $P = 4.43 \times 10^{-8}$ and 7.78×10^{-6} between iGluSnFR without or with Glu and 5-HT1.0 without 5-HT. $P = 4.62 \times 10^{-8}$ and 7.05×10^{-6} between iGluSnFR without or with Glu and 5-HT1.0 with 5-HT. **g**, Summary of the brightness measured in HEK293T cells expressing 5-HT1.0 or 5-HT2C-EGFP in the absence or presence of 10 μM 5-HT, normalized to the 5-HT2C-EGFP + 5-HT group; n = 3 wells per group with 300–500 cells per well. **h**,**i**, Intracellular calcium was measured in cells expressing 5-HT1.0 or the 5-HT2C receptor and loaded with the red fluorescent calcium dye Cal590. Representative traces are shown in (**h**), and the peak responses are plotted against 5-HT concentration in (**i**); n = 15/3 for each group. **j**,**k**, Fluorescence response of 5-HT1.0 expressing cells to 5-HT perfusion for two hours. Representative fluorescence images (**j**) and the summary data (**k**) showing the response to 10 μM 5-HT applied at 30 min intervals to cells expressing 5-HT1.0; n = 3 wells per group with 100-300 cells per well. Scale bar, 20 μm. $F_{4,10} = 0.888$, $P = 0.505$ for 0 min, 30 min, 60 min, 90 min and 120 min by one-way ANOVA. **l**, Left, the Gs-coupled cAMP level was detected by pink-Flamindo with or without 5-HT1.0 sensor expression. The exemplar fluorescence response traces of pink-Flamindo without (top) or with 5-HT1.0 sensor (bottom) expression, when treated with 50 μM 5-HT or 50 μM 5-HT + 10 μM Forskolin. Right, quantification data for left. n = 23/3, 23 cells from 3 cultures for each group. Two-tailed Student's t-test was performed. $P = 0.084$ and $P = 0.488$ for 5-HT and 5-HT + FSK group. **m**, Buffering effects of the 5-HT1.0 sensor by luciferase complementation assay. Luminescence signals were measured when treated with different concentrations of 5-HT (left) or 5-HT2C receptor specific agonist CP809101 (right) with or without co-expression of 5-HT1.0 sensor with 5-HT2C receptor. The luminescence signal of cells treated with the control buffer is normalized to 1. Data of 5-HT induced G-protein signaling in 5-HT2C receptor expression group were re-plotted from Fig. 1f. n = 3 wells per group with 100-300 cells per well. Two-tailed Student's t-test was performed. $P = 0.693$, 0.0402, 0.993, 0.340, 0.0618, 0.0691 and 0.127 between 5-HT1.0 and 5-HT1.0 + 5-HT2C with 10^{-4}, 10^{-5}, 10^{-6}, 10^{-7}, 10^{-8}, 10^{-9}, and 10^{-10} M 5-HT. $P = 0.733$, 0.801, 0.346, 0.998, 0.304 and 0.380 between 5-HT1.0 and 5-HT1.0 + 5-HT2C with 10^{-4}, 10^{-5}, 10^{-6}, 10^{-7}, 10^{-8} and 10^{-9} M CP809101. **n**, Cultured rat cortical neurons expressing the 5-HTmut sensor were imaged before (left) and after (middle) 5-HT application. These insets in the left and middle fluorescence images show the region with increased contrast. The pseudocolor image on the right shows the change in fluorescence of 5-HTmut in response to 10 μM 5-HT. Similar results were observed for more than 10 neurons. Scale bar, 20 μm. **o**,**p**, Representative trace (**o**) and group summary (**p**) of cultured neurons expressing 5-HT1.0 in response to indicated compounds at 10 μM each; in (**p**), Met was applied where indicated; n = 9/3. Two-tailed Student's t-test was performed. $P = 6.74 \times 10^{-22}$, 1.09×10^{-22}, 1.27×10^{-21}, 3.33×10^{-22}, and 0.0939 between 5-HT^{1st} and DA, NE, His, ACh and 5-HT^{2nd}. $P = 1.97 \times 10^{-11}$ between 5-HT^{2nd} and Met. Data are shown as the mean±s.e.m. in **b**-**d**, **f**, **g**, **i**, **k**-**m**, **p**, with the error bars or shaded regions indicating s.e.m., *$p < 0.05$, ** $p < 0.01$, ***$p < 0.001$, and n.s., not significant.

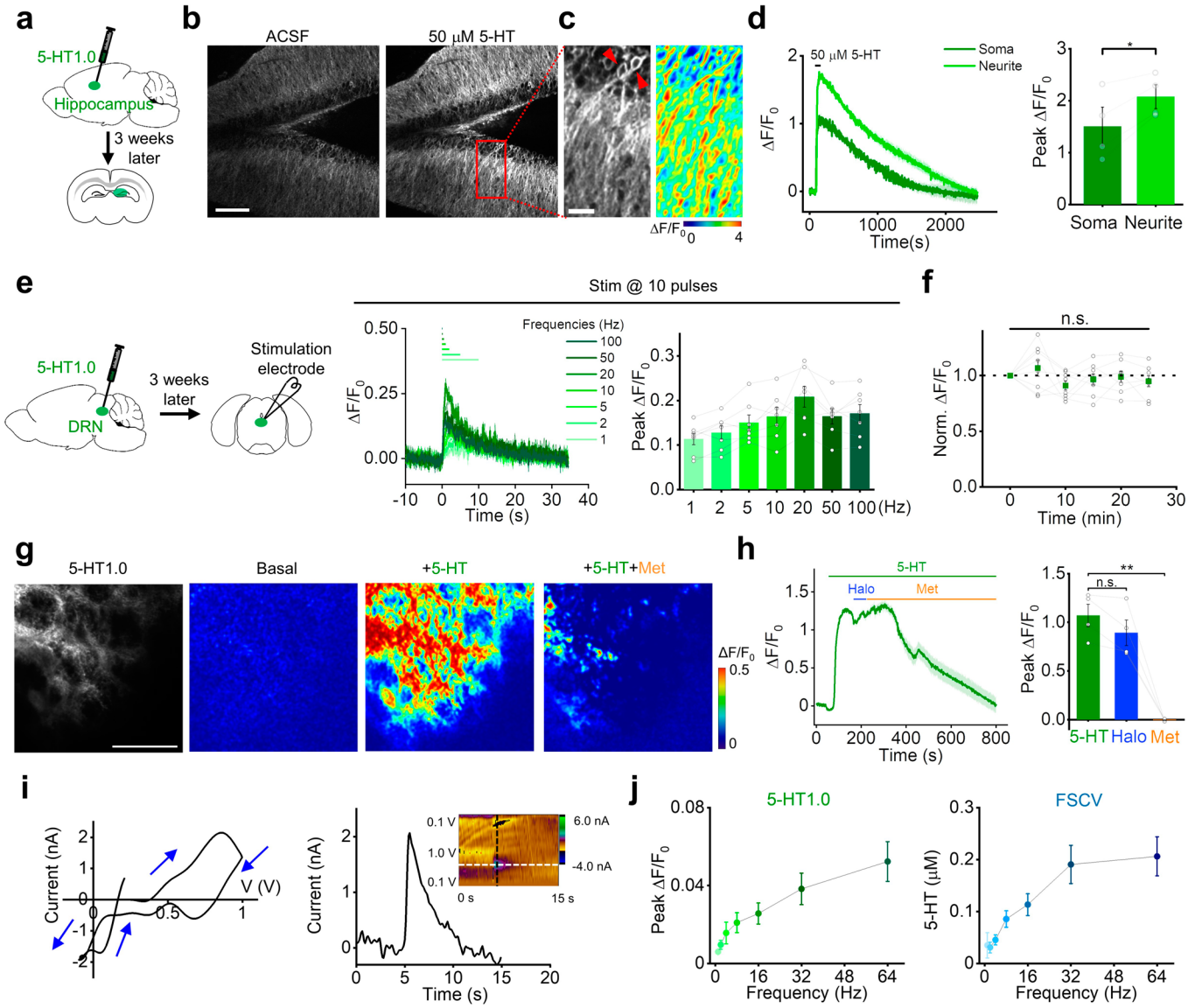

Extended Data Fig. 5 | Probing endogenous 5-HT release in mouse brain slices. a, Schematic diagram depicting the acute mouse brain slice preparation, with AAV-mediated expression of 5-HT1.0 in the hippocampus. **b**, Representative fluorescence images of the 5-HT1.0 sensor expressed in the mouse hippocampal neurons of brain slices in ACSF (left) and 50 μM 5-HT (right). Similar results were observed from 4 slices. Scale bar, 50 μm. **c**, A magnified view of the rectangular region in (b) showing the 5-HT1.0 sensor response to exogenously applied 50 μM 5-HT; left, fluorescence image; right, corresponding pseudocolor image indicating $\Delta F/F_0$. The arrowheads indicate somata. Scale bar, 15 μm. **d**, Representative traces (left) and quantification (right) of peak $\Delta F/F_0$ of the 5-HT1.0 sensor in response to 50 μM 5-HT from a single soma or neurite (n = 4 slices from 1 mouse). Two-tailed Student's t-test was performed. P = 0.0226 between soma and neurite. **e**, Left, schematic diagram depicting the acute mouse brain slice preparation, with AAV-mediated expression of 5-HT1.0 in the DRN. Middle and right, fluorescence traces (middle) and group data (right) of the change in 5-HT1.0 fluorescence in response to 10 electrical stimuli applied at the indicated frequencies; n = 7 slices from 5 mice. **f**, Summary of the change in 5-HT1.0 fluorescence in response to 6 trains of electrical stimuli (20 pulses at 20 Hz) delivered at 5-min intervals. The responses are normalized to the first train; n = 8 slices from 5 mice. $F_{5,42} = 1.18$, P = 0.335 for 0 min, 5 min, 10 min, 15 min, 20 min, and 25 min by one-way ANOVA. **g**,**h**, Representative fluorescence image, pseudocolor images (**g**), fluorescence traces (**h**, left), and group data (**h**, right) of 5-HT1.0 fluorescence in response to perfusion of 5-HT, 5-HT + Halo, and 5-HT + Met; n = 4 slices from 3 mice for each group. Two-tailed Student's t-test was performed. P = 0.0816 between 5-HT and Halo. P = 0.00297 between 5-HT and Met. **i**, Left, representative FSCV data of 5-HT release in DRN. A specific 5-HT waveform (0.2 V to 1.0 V and ramped down to −0.1 V, and back to 0.2 V at a scan rate of 1000 V/s) was applied to the CFME at a frequency of 10 Hz. Right, current vs time traces are extracted at a horizontal white dashed line shows an immediate increase in 5-HT response after electrical stimulation (20 pulses, 2 ms pulse width, 64 Hz). A cyclic voltammogram (inset) is extracted at the vertical black dashed line shows oxidation and reduction peaks at 0.8 V and 0 V, respectively. **j**, Left, group data of fluorescence response in 5-HT1.0-expressing DRN neurons to electrical stimuli with varied frequencies delivered at 20 pulses. Right, average data of peak 5-HT concentration measured by FSCV at varied stimulating frequencies delivered at 20 pulses; n = 11 neurons from 9 mice. Data are shown as the mean±s.e.m. in **d**-**f**, **h**, **j**, with the error bars or shaded regions indicating s.e.m., *p < 0.05, ** p < 0.01, ***p < 0.001, and n.s., not significant.

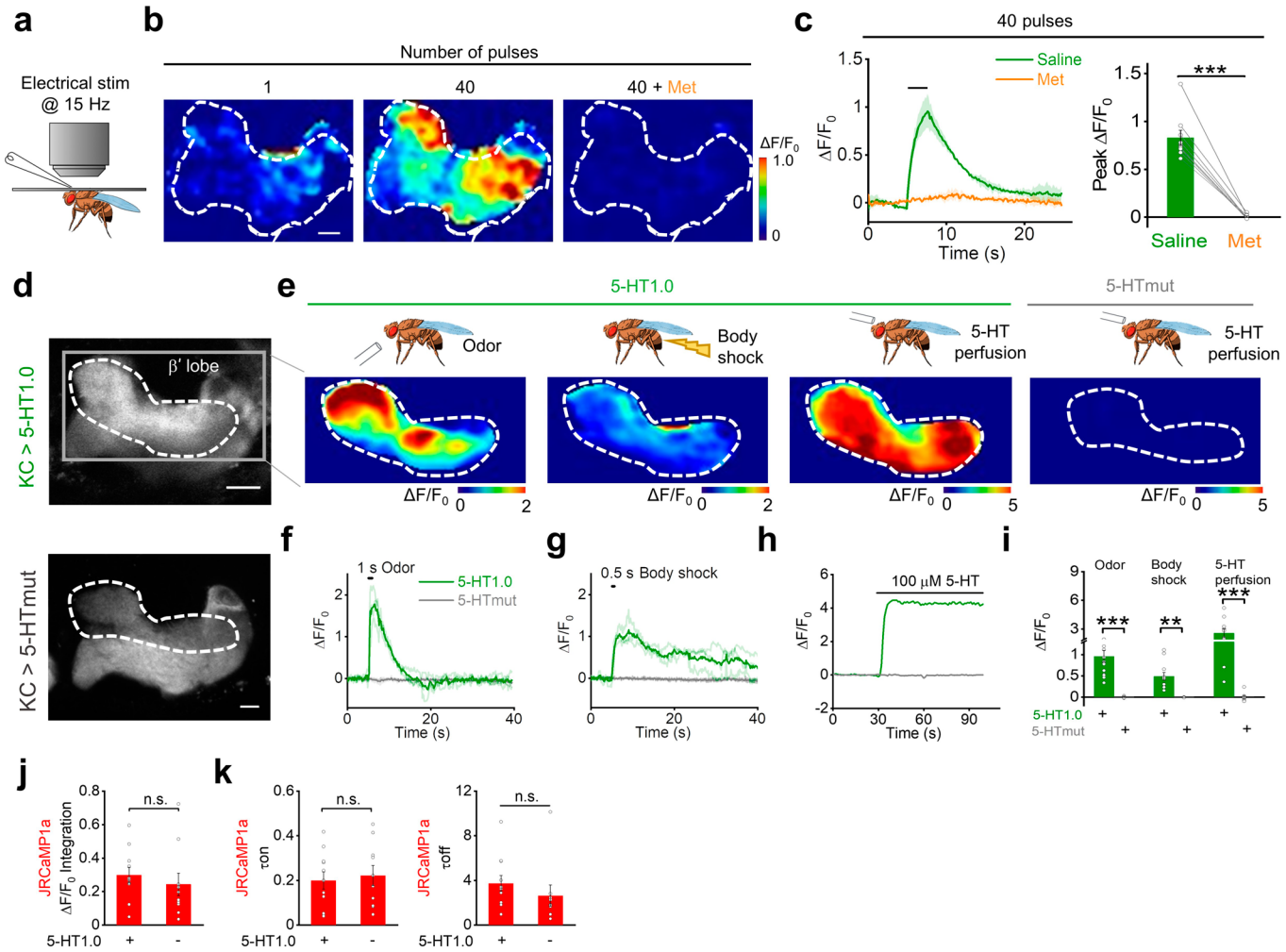

Extended Data Fig. 6 | Probing endogenous 5-HT release in *Drosophila in vivo*. a, Schematic drawing showing *in vivo* two-photon imaging of a *Drosophila*, with the stimulating electrode positioned near the mushroom body (MB). **b**,**c**, Representative pseudocolor images (**b**), fluorescence traces, and group summary (**c**) of the change in 5-HT1.0 fluorescence in the MB horizontal lobe in response to 40 electrical stimuli at 15 Hz in control (saline) or 10 μM Met; n = 9 flies for each group. Two-tailed Student's t-test was performed. $P = 2.36 \times 10^{-5}$ between saline and Met. Scale bar, 10 μm. **d**, Fluorescence images measured in the MB of flies expressing 5-HT1.0 or 5-HTmut; the β' lobe is indicated. Scale bar, 10 μm. **e-i**, Representative pseudocolor images (**e**), fluorescence traces (**f-h**), and group summary (**i**) of 5-HT1.0 and 5-HTmut in the MB β' lobe measured in response to a 1-s odor application, a 0.5-s body shock, and application of 100 μM 5-HT; n = 14, 12 and 10 flies for 5-HT1.0 group under odor, body shock and perfusion conditions; n = 9, 5 and 9 flies for 5-HTmut group under odor, body shock and perfusion conditions. Two-tailed Student's t-test was performed. $P = 1.14 \times 10^{-5}$, P = 0.00273, $P = 8.93 \times 10^{-5}$ between 5-HT1.0 and 5-HTmut under odor, body shock and perfusion conditions. **j**,**k**, Quantification data of area under the calcium transient curves (**k**) and the τon, τoff (**j**) in the main Fig. 2r,s; n = 11 and 10 flies for 5-HT1.0$^+$ and 5-HT1.0$^-$ group. Two-tailed Student's t-test was performed. P = 0.497 for calcium signal between two groups. P = 0.710 for τon and P = 0.307 for τoff. Data are shown as the mean ± s.e.m. in **c**, **i**-**k**, with the error bars or shaded regions indicating s.e.m., *p < 0.05, ** p < 0.01, ***p < 0.001, and n.s., not significant.

nature research

Corresponding author(s): Yulong Li

Last updated by author(s): Mar 18, 2021

Reporting Summary

Nature Research wishes to improve the reproducibility of the work that we publish. This form provides structure for consistency and transparency in reporting. For further information on Nature Research policies, see our Editorial Policies and the Editorial Policy Checklist.

Statistics

For all statistical analyses, confirm that the following items are present in the figure legend, table legend, main text, or Methods section.

n/a	Confirmed	
☐	☒	The exact sample size (*n*) for each experimental group/condition, given as a discrete number and unit of measurement
☐	☒	A statement on whether measurements were taken from distinct samples or whether the same sample was measured repeatedly
☐	☒	The statistical test(s) used AND whether they are one- or two-sided *Only common tests should be described solely by name; describe more complex techniques in the Methods section.*
☒	☐	A description of all covariates tested
☐	☒	A description of any assumptions or corrections, such as tests of normality and adjustment for multiple comparisons
☐	☒	A full description of the statistical parameters including central tendency (e.g. means) or other basic estimates (e.g. regression coefficient) AND variation (e.g. standard deviation) or associated estimates of uncertainty (e.g. confidence intervals)
☐	☒	For null hypothesis testing, the test statistic (e.g. *F*, *t*, *r*) with confidence intervals, effect sizes, degrees of freedom and *P* value noted *Give P values as exact values whenever suitable.*
☒	☐	For Bayesian analysis, information on the choice of priors and Markov chain Monte Carlo settings
☒	☐	For hierarchical and complex designs, identification of the appropriate level for tests and full reporting of outcomes
☒	☐	Estimates of effect sizes (e.g. Cohen's *d*, Pearson's *r*), indicating how they were calculated

Our web collection on statistics for biologists contains articles on many of the points above.

Software and code

Policy information about availability of computer code

Data collection	The Harmony software of Opera Phenix high-content screening system (PerkinElmer). The NIS-Element software of Ti-E A1 confocal microscope (Nikon). The FV10-ASW software of FV1000MPE 2-photon microscope (Olympus). The commercial software of the photometry system (TDT).
Data analysis	Matlab R2020a (MathWorks) and ImageJ 1.52p (NIH) software were used for imaging data processing, and data was plotted in Origin 2020b (OriginLab). EZcalcium algorism. https://github.com/porteralab/EZcalcium. BEADS baseline estimation and denoising with sparsity algorism. https://www.mathworks.com/matlabcentral/fileexchange/49974-beads-baseline-estimation-and-denoising-with-sparsity.

For manuscripts utilizing custom algorithms or software that are central to the research but not yet described in published literature, software must be made available to editors and reviewers. We strongly encourage code deposition in a community repository (e.g. GitHub). See the Nature Research guidelines for submitting code & software for further information.

Data

Policy information about availability of data

All manuscripts must include a data availability statement. This statement should provide the following information, where applicable:

- Accession codes, unique identifiers, or web links for publicly available datasets
- A list of figures that have associated raw data
- A description of any restrictions on data availability

The plasmid pAAV-hSyn-GRAB5-HT1.0 (#140552) has been deposited to Addgene database. Source data are provided with this paper.

Field-specific reporting

Please select the one below that is the best fit for your research. If you are not sure, read the appropriate sections before making your selection.

☒ Life sciences ☐ Behavioural & social sciences ☐ Ecological, evolutionary & environmental sciences

For a reference copy of the document with all sections, see nature.com/documents/nr-reporting-summary-flat.pdf

Life sciences study design

All studies must disclose on these points even when the disclosure is negative.

Sample size	No statistical methods were used to predetermine sample size. We used similar sample sizes to the literatures in the field. [1] Jing, Miao, et al. "A genetically encoded fluorescent acetylcholine indicator for in vitro and in vivo studies." Nature biotechnology 36.8 (2018): 726-737. [2] Sun, F., Zeng, J., Jing, M., Zhou, J., Feng, J., Owen, S. F., ... & Li, Y. (2018). A genetically encoded fluorescent sensor enables rapid and specific detection of dopamine in flies, fish, and mice. Cell, 174(2), 481-496. [3] Patriarchi, Tommaso, et al. "Ultrafast neuronal imaging of dopamine dynamics with designed genetically encoded sensors." Science 360.6396 (2018). [4] Feng, Jiesi, et al. "A genetically encoded fluorescent sensor for rapid and specific in vivo detection of norepinephrine." Neuron 102.4 (2019): 745-761.
Data exclusions	No data were excluded for the analysis.
Replication	Each experiment in this manuscript is reliably reproduced. The replication number of each experiment is indicated in the legend of corresponding figures.
Randomization	Animals or cells were randomly assigned into control or experimental groups.
Blinding	The investigators were not blind to group allocation during data collection and analysis. The experimental conditions were obvious to the researchers and the analysis were performed objectively and not subjective to human bias.

Reporting for specific materials, systems and methods

We require information from authors about some types of materials, experimental systems and methods used in many studies. Here, indicate whether each material, system or method listed is relevant to your study. If you are not sure if a list item applies to your research, read the appropriate section before selecting a response.

Materials & experimental systems

n/a	Involved in the study
☐	☒ Antibodies
☐	☒ Eukaryotic cell lines
☒	☐ Palaeontology and archaeology
☐	☒ Animals and other organisms
☒	☐ Human research participants
☒	☐ Clinical data
☒	☐ Dual use research of concern

Methods

n/a	Involved in the study
☒	☐ ChIP-seq
☒	☐ Flow cytometry
☒	☐ MRI-based neuroimaging

Antibodies

Antibodies used	Primary antibody: (1) Rabbit anti-mCherry antibody (1:500) (Abcam) (Cat#: ab167453). Secondary antibody: (1) AlexFlour647 goat anti-rabbit (1:500) (AAT Bioquest) (Cat#: 16710).
Validation	The Rabbit anti-mCherry antibody (Abcam, Cat#ab167453) used in immunohistochemistry has been verified in Bonaventura, Jordi, et al, Nature Communications 10.1 (2019): 4627-4627. The AlexFlour647 goat anti-rabbit antibody (AAT Bioquest, Cat#: 16710) used in immunohistochemistry has been verified in Zhao, Jingkun, et al, Oncotarget 8.17 (2017): 28442-28454.

Eukaryotic cell lines

Policy information about cell lines

Cell line source(s)	HEK293T cells used in this paper were purchased from ATCC. The HEK293 cell line stably expressing a tTA-dependent luciferase reporter and the β-arrestin2-TEV fusion gene used in the TANGO assay was a generous gift from Bryan L. Roth.

Authentication	We have verified the cell line based on their morphology under microscope and an analysis of their growth curve.
Mycoplasma contamination	No mycoplasma contamination.
Commonly misidentified lines (See ICLAC register)	No commonly misidentified cell lines were used.

Animals and other organisms

Policy information about studies involving animals; ARRIVE guidelines recommended for reporting animal research

Laboratory animals	The following fly stocks were used in this study: R13F02-Gal4 (BDSC:48571), UAS-jRCaMP1a (BDSC: 63792), VT64246-Gal4 (VDSC:204311) UAS-GRAB5-HT1.0 (attp40, UAS-GRAB5-HT1.0/CyO) and UAS-GRAB5-HTmut (attp40, UAS-GRAB5-HTmut/CyO). Adult male flies within two weeks post eclosion were used for imaging, and their genotypes have been declared in the methods. Male and female postnatal day 0 (P0) Sprague-Dawley rat pups were used to prepare cortical neurons. Male and female wild-type C57BL/6N (P25-60) mice were used to prepare the acute brain slices and for the in vivo mouse experiments.
Wild animals	No wild animals were used in the study.
Field-collected samples	No field-collected samples were used in the study.
Ethics oversight	All procedures for animal surgery and maintenance were performed using protocols that were approved by the Animal Care & Use Committees at Peking University, the Chinese Academy of Sciences, University of Virginia, and were performed in accordance with the guidelines established by the US National Institutes of Health.

Note that full information on the approval of the study protocol must also be provided in the manuscript.